Journal Pre-proofs

Observer-Based Incremental Backstepping Sliding-Mode Fault-Tolerant Control for Blended-wing-body Aircrafts

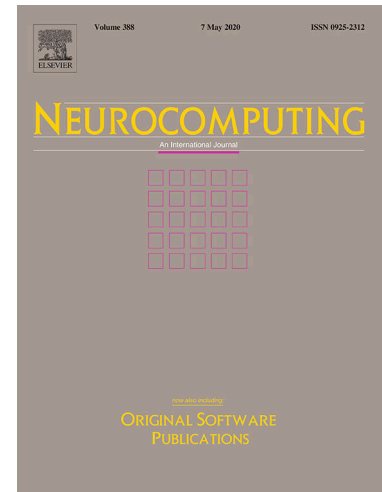Shi Qian Liu, James F. Whidborne

Please cite this article as: S. Qian Liu, J.F. Whidborne, Observer-Based Incremental Backstepping Sliding-Mode Fault-Tolerant Control for Blended-wing-body Aircrafts, *Neurocomputing* (2021), doi: https://doi.org/10.1016/j.neucom.2021.08.069

Observer-Based Incremental Backstepping Sliding-Mode Fault-Tolerant Control for Blended-wing-body Aircrafts

Shi Qian Liu[1], James F. Whidborne[2]

[1] *School of Aeronautics and Astronautics, Shanghai Jiao Tong University, Shanghai 200240, China*

[2] *School of Aerospace, Transport and Manufacturing, Cranfield University, Cranfield MK43 0AL, UK*

ABSTRACT

This paper presents an adaptive incremental nonlinear backstepping sliding-mode (INBSM) controller, for fault tolerant tracking control of a blended wing body (BWB) aircraft with unknown disturbances and actuator faults. The INBSM controller is based on a nonlinear dynamics model of the BWB aircraft. In addition, a radial basis function neural network disturbance observer (RBF-NNDO) is proposed to enhance the disturbance attenuation ability. A fault estimator is suggested to improve actuator fault tolerant control level. The closed-loop control system of the BWB aircraft is proved to be globally asymptotically stable using Lyapunov theory. Simulations of the combined NNDO-INBSM controller are presented and compared with both the INBSM design and an adaptive fuzzy controller. The results demonstrate an improved capability of the NNDO-INBSM control for the BWB aircraft to execute realistic attitude tracking missions, even in the presence of center of gravity movement, unknown disturbances, model uncertainties and actuator faults.

Keywords: Robust control of nonlinear system; neural network disturbance observer; incremental nonlinear backstepping control; incremental nonlinear dynamic inversion; stability augmentation control

E-mail addresses: liushiqian@sjtu.edu.cn (S.Q. Liu), j.f.whidborne@cranfield.ac.uk (J.F. Whidborne)

1. Introduction

The blended wing body aircraft is a creative airframe design which seamlessly combines a flying wing with a futuristic fuselage. It has potential advantages in lower carbon emissions, reduction of noise, higher speed, longer flight range, and broader internal volume [1, 2]. However, due to the flying wing configuration, the longitudinal stability of the BWB aircraft decreases as the angle of attack increases, even at small angles of attack. This is because the lift curve shows a nonlinear increase at small angles of attack because of flow separation [3,4], and the nonlinear change of pitching moment can easily make the BWB aircraft unstable due to the aerodynamic center moving forward. Furthermore, because the pitch arm of the BWB aircraft is shorter than that of classical configurations, the pitch trim ability of the BWB aircraft is insufficient when climbing at low speed and high angle of attack. These make the BWB aircraft design and flight control very challenging [5].

Qin and Vavalle initially studied the lift distribution of the BWB aircraft [6]. Castro studied the control stability augmentation and flying qualities of a BWB aircraft designed by Cranfield University [7]. Rahman & Whidborne proposed an integration strategy of propulsion and flight control for the BWB aircraft [8]. Yann and Joël studied multi-control surface optimization for the BWB aircraft under handling quality constraints [9]. However, most of these modelled the BWB aircraft as a linear time-invariant system and then used conventional linear control methods to design controllers.

To improve the control performance of an aircraft with nonlinear models, many nonlinear control methods have been studied, backstepping and feedback linearization are two common methods [10]. Liu and Sang proposed both backstepping and sliding mode backstepping control to realize trajectory tracking control of stratospheric airships [11-15]. Bacon and Ostroff expanded dynamic inversion into an incremental form by introducing an angular acceleration feedback [16]. Incremental nonlinear

dynamic inversion (INDI), a method in which the dynamics are written in an incremental form, is a sensor-based control method that does not rely on accurate aircraft model, and it can realize aircraft's flight under certain uncertainties and structural faults [17]. Smeur, Chu *et al*. used an adaptive incremental nonlinear dynamic inversion to control the attitude of a miniature unmanned aerial vehicle (UAV) [18]. Recently Lu and Kampen proposed a fault tolerant trajectory tracking control based on INDI to deal with actuator faults [19], and Wang and Kampen proposed a combination of sliding mode control and incremental aerodynamic dynamic inversion, so that the gain of the sliding mode controller could be reduced while making up for the remaining perturbations [20]. Incremental backstepping control is another form of incremental nonlinear control which brings the implicitness of sensor-based architectures with Lyapunov-based control design [21]. Ali, Chu *et al*. proposed an adaptive INBS using immersion and invariance to control an F-16 aircraft [22]. Lu and Kampen studied the robustness problem of attitude control by using INBS [23]. Wang and Chen used a command-filtered incremental backstepping controller to realize a small UAV attitude control and improved the plant robustness [24].

Since aircraft are subjected to unknown disturbances such as wind and turbulence, a nonlinear disturbance observer-based control (DOBC) approach is introduced here to enhance the disturbance attenuation capability of the INBSM control. The disturbance observer-based technique has been applied to the nonlinear systems with unknown disturbances for three decades [25], where an observer is designed to estimate external disturbances and then compensate for them [26]. Recently a fuzzy disturbance observer and a neural network disturbance observer have been developed and applied to position systems and UAVs [27-28]. Meanwhile, neural networks, with strong approximation capacities, can be employed for robust control by combining with backstepping, thus model uncertainty and disturbances are all handled [29].

Motivated by the weak static stability of blended wing body aircraft that make it sensitive to unknown wind and faults, and by the work of Castro [7], Acquatella and Chu [21], Chen [25] and Zheng [29], this paper mainly concerns the stability augmentation system and attitude tracking control for a BWB aircraft with unknown disturbances, model uncertainties and actuator faults. The main contributions are listed as follows. The stability augmentation system to improve dynamic stability characteristics for the BWB aircraft with nonlinear motions is studied. The influence of center of gravity (CG) position on the BWB aircraft stability is analyzed. The stability enhancement or large stability margins by using INBSM control and adaptive fuzzy control will be proved and numerically verified when the system has uncertainties or time delays. A novel RBF NNDO enhanced INBSM is proposed for the attitude tracking. An NNDO based approach is applied to enhance its disturbance attenuation capability and provide robustness against model uncertainties. The uncertainties of the dynamics and unobservable disturbances are compensated by using a robust adaptive RBF-NN. The INBSM method is used to realize robustness attitude tracking control. The NNDO observer is designed for aerodynamic coefficient uncertainty and unknown environmental disturbances, and the fault estimator is proposed for the actuator fault tolerant control.

This paper is organized as follows. Section 2 gives the nonlinear dynamics model of the BWB aircraft and presents the stability augmentation and attitude tracking problem. Section 3 proposes a nonlinear NNDO-INBSM control design, and stability is analyzed for the associated closed-loop tracking error system. Simulations and performances of three scenarios with the NNDO-INBSM control method are demonstrated in Section 4. Section 5 gives some conclusions.

2. Dynamics modeling and problem formulation

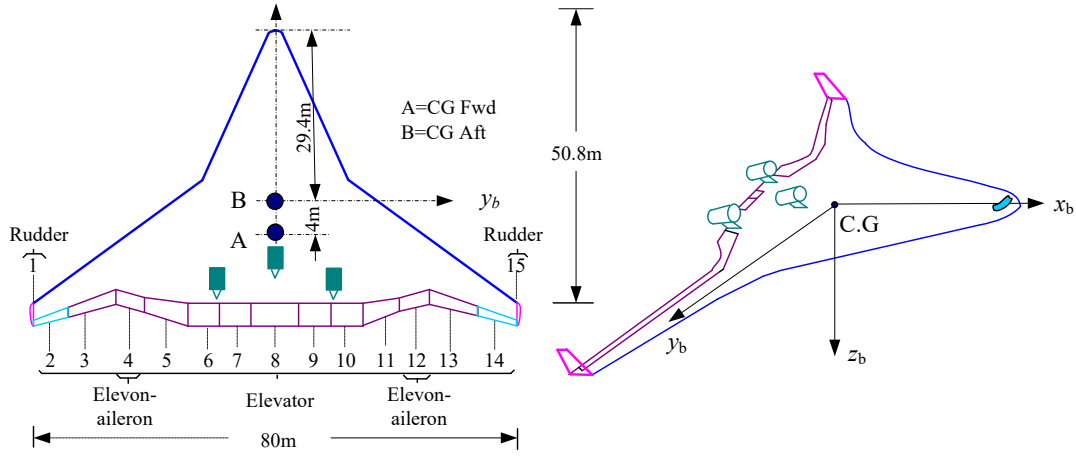### 2.1 Dynamics modeling of the BWB aircraft

Fig.1 The BWB aircraft platform and geometry

The BWB aircraft is shown Fig.1. It is a flying-wing configuration with 50.8m length and 80m wing span, and has fifteen flaps. Flap 1 and Flap 15 are rudders, which are not in the wing plane. Flap 12 and Flap 4 are elevon-ailerons, while Flaps 2 –14 are the elevators. The aircraft is considered as a rigid body moving in air. The dynamics model is established as follows

$$
\begin{bmatrix} \dot{u} \\ \dot{v} \\ \dot{w} \end{bmatrix} = \begin{pmatrix} -qw+rv \\ -ru+pw \\ -pv+qu \end{pmatrix} + g \begin{bmatrix} -\sin\theta \\ \cos\theta\sin\phi \\ \cos\theta\cos\phi \end{bmatrix} + \frac{1}{m} \begin{bmatrix} \bar{q}SC_{xa} \\ \bar{q}SC_{ya} \\ \bar{q}SC_{za} \end{bmatrix} + \frac{1}{m} \begin{bmatrix} \bar{q}SC_{x\delta}+T \\ \bar{q}SC_{y\delta} \\ \bar{q}SC_{z\delta} \end{bmatrix} \tag{1}
$$

$$
\begin{bmatrix} \dot{p} \\ \dot{q} \\ \dot{r} \end{bmatrix} = -\bar{I}^{-1} \begin{bmatrix} p \\ q \\ r \end{bmatrix} \times \left(\bar{I} \begin{bmatrix} p \\ q \\ r \end{bmatrix} \right) + \bar{I}^{-1} \begin{bmatrix} \bar{q}SbC_{la} \\ \bar{q}S\bar{c}C_{ma} \\ \bar{q}SbC_{na} \end{bmatrix} + \bar{I}^{-1} \begin{bmatrix} \bar{q}SbC_{l\delta} \\ \bar{q}S\bar{c}C_{m\delta} \\ \bar{q}SbC_{n\delta} \end{bmatrix} \tag{2}
$$

where T denotes thrust, $C_x, C_y, C_z, C_l, C_m, C_n$ are aerodynamic force coefficients and moment coefficients as referred in [7, 8], subscripts a and δ denote aerodynamic terms of surfaces without control and of control surfaces respectively. $V = [u\ v\ w]^T$ is the body-fixed velocity, the position in the flat earth axes is $\boldsymbol{\xi} = [x\ y\ z]^T$, $\boldsymbol{\omega} = [p\ q\ r]^T$ is the body-fixed rotational rare, $\boldsymbol{\eta} = [\ \phi\ \ \theta\ \psi]^T$ is the aircraft attitude, m is the mass of the BWB aircraft, and $\bar{\boldsymbol{I}} = \begin{bmatrix} I_{xx} & -I_{xy} & -I_{xz} \\ -I_{xy} & I_{yy} & -I_{yz} \\ -I_{xz} & -I_{yz} & I_{zz} \end{bmatrix}$ is the aircraft inertial moment matrix.

Now consider the attitude motion of the BWB aircraft. Denote $x^T = \begin{bmatrix} x_1 & x_2 \end{bmatrix}$ as the state vector, where $x_1 = \eta$, $x_2 = \omega$, the attitude motion model of the BWB aircraft can be rewritten as follows [17],

$$\dot{x}_1(t) = J(\eta) x_2(t) \tag{3a}$$

$$\dot{x}_2(t) = f_2 + G_2 u \tag{3b}$$

where $f_2(\,\cdot\,)$ and $G_2(\,\cdot\,)$ are continuous mapping functions as

$$f_2 = -\overline{I}^{-1} \begin{bmatrix} p \\ q \\ r \end{bmatrix} \times \left(\overline{I} \begin{bmatrix} p \\ q \\ r \end{bmatrix} \right) + \overline{I}^{-1} \begin{bmatrix} \overline{q}SbC_{la} \\ \overline{q}S\overline{c}C_{ma} \\ \overline{q}SbC_{na} \end{bmatrix}, \tag{4}$$

$$G_2 = \overline{I}^{-1} (M_c)_\delta, \quad M_c = \begin{bmatrix} \overline{q}Sb\left(C_{l_{\delta a}}\delta_a + C_{l_{\delta r}}\delta_r\right) \\ \overline{q}S\overline{c}C_{m_{\delta e}}\delta_e \\ \overline{q}Sb\left(C_{n_{\delta_r}}\delta_r + C_{n_{\delta a}}\delta_a\right) \end{bmatrix}, \quad (M_c)_\delta = \frac{\partial M_c}{\partial \delta} = \overline{q}S \begin{bmatrix} C_{l_{\delta a}} & 0 & C_{l_{\delta_r}} \\ 0 & C_{m_{\delta e}} & 0 \\ C_{n_{\delta a}} & 0 & C_{n_{\delta_r}} \end{bmatrix} \begin{pmatrix} b \\ \overline{c} \\ b \end{pmatrix} \tag{5}$$

where $\overline{q}$ denotes dynamic pressure, S is reference area of the wing, b and $\overline{c}$ are wing span and mean aerodynamic chord length of the wing, $C_{l_{\delta_a}}$, $C_{m_{\delta_e}}$ and $C_{n_{\delta_r}}$ denote aerodynamic derivative coefficients of the aileron, elevator and rudder respectively. The transformation matrix J is

$$J(\eta) = \begin{pmatrix} 1 & s(\phi)\tan\theta & c(\phi)\tan\theta \\ 0 & c(\phi) & -s(\phi) \\ 0 & s(\phi)\sec\theta & c(\phi)\sec\theta \end{pmatrix} \tag{6}$$

where $|\theta| < \pi/2$ is assumed to avoid the singularity of the matrix because $\theta = \pm\pi/2$ is not likely to be encountered during practical operation of the aircraft, $s(\ )$ and $c(\ )$ denote the sine and cosine functions respectively.

Disturbances widely exist and act on the BWB aircraft, which adversely affect the performance and stability of the flight control system. The disturbance includes modelling errors caused by the uncertainty as well as the disturbances from the external environment. Since the disturbance is difficultly measured by sensors, then disturbance rejection becomes one challenge of the control system design. So the model uncertainty and external disturbance $D = \begin{bmatrix} D_V^T & D_\omega^T \end{bmatrix}^T$ are introduced

meeting with $|\boldsymbol{D}| < \boldsymbol{D}_\text{U}$, where $\boldsymbol{D}_\text{U}$ is a real value, and the system of (3) can be modified in an affine

form,

$$\dot{\boldsymbol{x}}_2(t) = \boldsymbol{f}_2 + G_2\boldsymbol{u} + g_{d_\omega}\boldsymbol{D}_\omega \tag{7}$$

where $\boldsymbol{D}_\omega \in \mathbb{R}^3$ denotes the attitude disturbance vector, assume $\boldsymbol{D}_\omega$ is bounded, $g_{d_\omega}(\boldsymbol{x}) = \overline{\boldsymbol{I}}^{-1}$.

2.2 The attitude tracking control problem

Consider the BWB aircraft models of (3) and (7). Let $\boldsymbol{\eta}_d(t):[0,\infty) \to \mathbb{R}^3$ be a given, sufficiently

smooth, time-varying reference attitude with bounded time-derivatives of ($\dot{\boldsymbol{\eta}}_d(t)$, $\ddot{\boldsymbol{\eta}}_d(t)$). The control

task is to design a nonlinear controller such that the closed-loop system meets following requirements:

1) Stability of the closed-loop system is enhanced when the center of gravity (CG) of the BWB

aircraft moves aftwards;

2) The attitude tracking error dynamics of the BWB aircraft are globally asymptotically stable under

specified model uncertainty, external disturbances and actuator faults.

3   NNDO-INBSM augmentation control design

This section gives an overview of the NNDO-INBSM control for the BWB aircraft. The proposed

controller structure is shown in Fig.2, which includes an augmentation control, a NN disturbance

observer, an incremental backstepping sliding mode control, a fault estimator and the BWB aircraft

dynamics model. The INBSM controller is there to realize the attitude tracking, and the NNDO to

observe the observable disturbances; the unobservable disturbances can be approximated by the neural

network. The stable filter and command filter are applied to suppress high frequency signal inputs. The

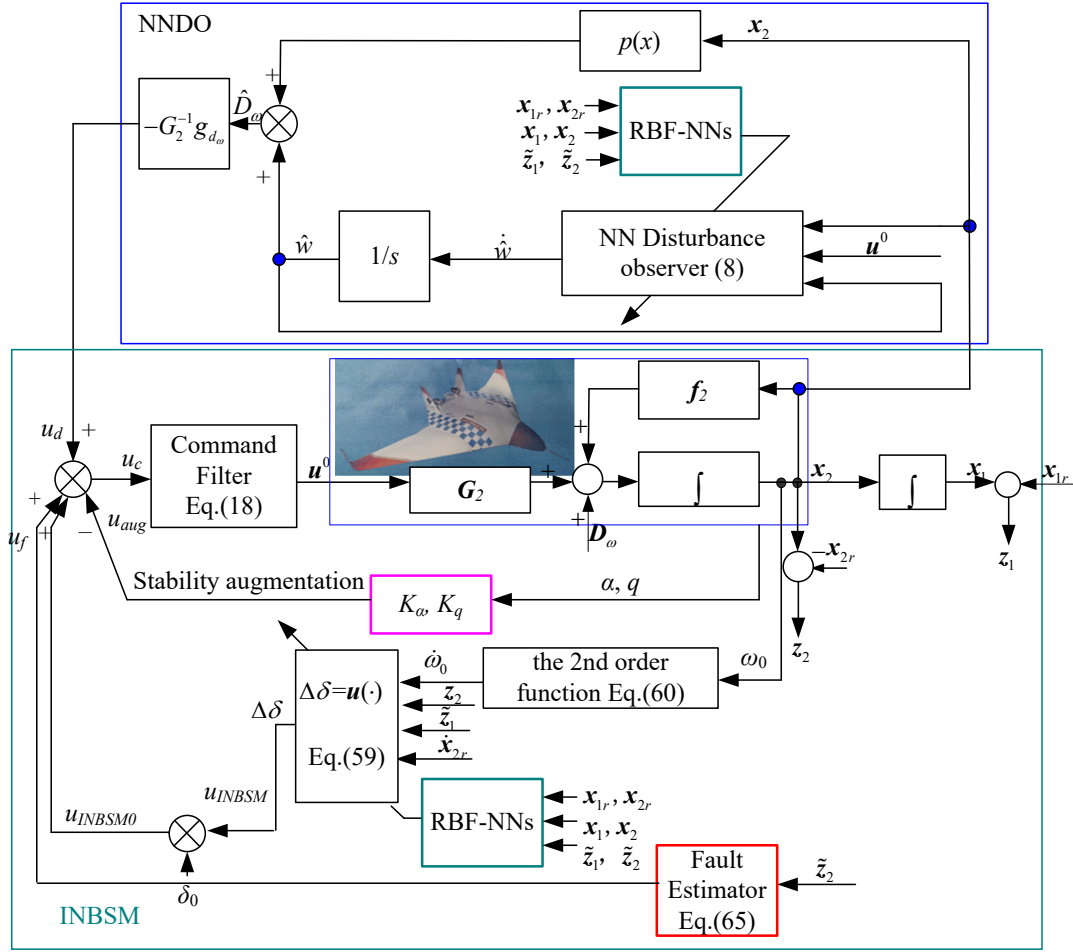controller design is presented in detail in the next section.

Fig.2 Block of the NNDO-INBSM controller for the BWB aircraft

3.1 Neural-Network Disturbance Observer Design

Since the tracking control system for (7) has the unknown bounded disturbance D_ω, a neural-network disturbance observer is designed to improve the tracking precision [25, 30],

$$
\begin{cases}
\dot{\hat{w}}(t) = -l(x)g_{d_\omega}(x)\hat{w}(t) - l(x)\Big(g_{d_\omega}(x)p(x) + f_2(x) + G_2 u + \hat{W}^T h(x)\Big) \\
\hat{D}_\omega(t) = \hat{w}(t) + p(x)
\end{cases}
\tag{8}
$$

where $\hat{w} \in \mathbb{R}^3$ is the internal state of the nonlinear observer, $\hat{D}_\omega$ is the estimation of D_ω, $\hat{W}$ is the estimation of the best weight vector of the RBF neural network, $h(x)$ is the basis function as in (14), and $p(x)$ is the nonlinear function to be designed.

The advantages of the RBF-NNDO are that not only unknown disturbances can be estimated, but also model uncertainties can be approximated by the radial basis function neural network, thus the

disturbance attenuation ability is greatly enhanced. The NNDO gain $l(x)$ is determined by

$$l(x) = \frac{\partial p(x)}{\partial x} \tag{9}$$

It has been shown in [25] that the NNDO asymptotically estimates the disturbance if the observer gain $l(x)$ is chosen such that the following error plant (10) is asymptotically stable.

$$
\begin{aligned}
\dot{d}_\omega = \dot{D}_\omega - \dot{\hat{D}}_\omega = -\dot{\hat{D}}_\omega &= -\dot{\hat{w}}(t) - \frac{dp(x)}{dt} \\
&= l(x)g_{d_\omega}(x)\hat{w}(t) + l(x)\Big(g_{d_\omega}(x)p(x) + f_2(x) + G_2(x)u\Big) - \frac{dp(x)}{dt} \\
&= l(x)\hat{D}_\omega - l(x)D_\omega \\
&= -l(x)g_{d_\omega}d_\omega
\end{aligned}
\tag{10}
$$

where $d_\omega = D_\omega - \hat{D}_\omega$ denotes the unobservable part of the overall disturbance D_ω.

Remark 1 The design of a disturbance observer (8) essentially is to choose an appropriate gain $l(x)$ and associated $p(x)$ such that the convergence of estimation error d_ω is guaranteed. It is possible to choose $l(x)$ as a constant matrix such that all the eigenvalues of matrix $-l(x)g_{d_\omega}$ have negative real parts. Multiplying $l(x)$ with the aircraft state x yields $p(x) = l(x)\,x$.

It has been shown that the estimation $\hat{D}_\omega(t)$ of the NNDO approaches the disturbance $D_\omega(t)$ exponentially, if the observer gain $l(x)$ is chosen such that the error system (10) is global exponentially stable for all $x \in \mathbb{R}^n$ [25]. Hence the disturbance compensator can be designed as

$$u_d = -G_2^{-1}\Big(g_{d_\omega}\hat{D}_\omega\Big) \tag{11}$$

By using the proposed nonlinear disturbance observer, the disturbance D_ω has been reduced and the system (7) can be transformed as follows:

$$
\begin{aligned}
\dot{x}_2(t) &= f_2(x) + G_2(x)\big(u_{INBS} + u_d\big) + g_{d_\omega}D_\omega \\
&= f_2(x) + G_2(x)u_{INBS}(t) + g_{d_\omega}d_\omega(t)
\end{aligned}
\tag{12}
$$

Usually suppose that the unobservable disturbance d_ω varies slowly relative to the observer

dynamics, i.e. $\dot{d}_{\omega} \approx 0$, so this will produce conservative control, to break this assumption and reduce

this conservativeness, in this paper a neural network is used to approximate this disturbance as follows

$$\dot{x}_2(t) = f_2(x) + G_2(x)u_{INBS}(t) + \left(W^{*T} \cdot h(x) + \varepsilon\right) \tag{13}$$

where W^* denotes the optimal weight matrix of the RBF-NN, ε is approximation error, which can be

arbitrarily small variable by regulating the weight and nodes of the RBF-NN, so we assume that

$|\varepsilon| \le \bar{\varepsilon}$, $\bar{\varepsilon} > 0$. The output of the neural network is $h(x) = \left[h_j(x)\right]^T$, $h(x)$ is the basis function which

can be selected as following Gaussian function

$$h_j(x) = \exp\left(\frac{\|x - c_j\|^2}{2b_j^2}\right) \tag{14}$$

where c_j is the centre value of neural net j, b_j is the width value of the Gaussian function of net j, j is

the node number of the hidden layer. The disturbance term of $\dot{d}_{\omega}t$ is approximated by

$y_{NN} = W^{*T} \cdot h(x) + \varepsilon$.

The faults of the aircraft actuators can be modeled as [31]

$$\boldsymbol{u}_a(t) = \boldsymbol{u}(t) + (\boldsymbol{I} - \bar{\boldsymbol{\rho}}_a(t))\left(\boldsymbol{f}_a(t) - \boldsymbol{u}_a(t)\right) \tag{15}$$

that is,

$$\boldsymbol{u}_c(t) = \boldsymbol{u}_a(t) = \bar{\boldsymbol{\rho}}_a \boldsymbol{u}(t) + (\boldsymbol{I} - \bar{\boldsymbol{\rho}}_a(t))\boldsymbol{f}_a(t) \tag{16}$$

where $\boldsymbol{u}_a = \left[u_{a,1}, u_{a,2}, \cdots, u_{a,m}\right] \in \mathbb{R}^m$ is the actual control output, $\boldsymbol{u} \in \mathbb{R}^m$ is the synthesized control

output, the diagonal matrix $\bar{\boldsymbol{\rho}}_a = \mathrm{diag}\left\{\rho_{a,1}, \rho_{a,2}, \cdots, \rho_{a,m}\right\}$ denotes the operational effectiveness of the

actuators, $\boldsymbol{I}$ is $m \times m$ identity matrix, the fault vector $\boldsymbol{f}_a = \left[f_{a,1}, f_{a,2}, \cdots, f_{a,m}\right] \in \mathbb{R}^m$ denotes stuck, or

floating value of the actuators. Since fault compensation mainly relies on the INBS control, so

$\boldsymbol{u}_{INBS}(t) \approx \boldsymbol{u}_a(t)$ and substituting Eq.(16) into Eq.(13) yields

$$\dot{\boldsymbol{x}}_2(t) = \boldsymbol{f}_2(t) + G_2\bar{\boldsymbol{\rho}}_a\boldsymbol{u}(t) + G_2(\boldsymbol{I} - \bar{\boldsymbol{\rho}}_a(t))\boldsymbol{f}_a(t) + W^{*T} \cdot h(x) + \varepsilon \tag{17}$$

3.2. Backstepping stability augmentation and attitude control

This section is to design the backstepping controller, and the objective is to make the closed-loop system stability augmentation and the attitude output $\boldsymbol{\eta}$ converge to the desired value vector $\boldsymbol{\eta}_d$.

A command filter is used to meet magnitude and rate constraints of the input signal. The command filter can be obtained by using a second-order lower pass filter as follows

$$G_r(s) = \frac{X_r(s)}{X_r^0(s)} = \frac{\omega_n^2}{s^2 + 2\zeta_n \omega_n s + \omega_n^2} \tag{18}$$

where ζ_n denotes the filter damping ratio, ω_n denotes the filter nature frequency. To reduce the filter error $e_r \triangleq x_r^0 - x_r$, the filter frequency ω_n is the bandwidth of $X_r^0(s)$, which is generally less than that of $G_r(s)$, and then ω_n can be selected.

Due to mass and passenger changes, the position of CG of the BWB aircraft changes. When the CG position of the aircraft moves aftwards, the stability of the BWB aircraft decreases. To implement augmentation control, usually the angle of attack (AOA, α) and pith rate (q) are selected as the feedback signals to implement pitch-axis stability[32], but the BWB aircraft is sensitive for AOA, the feedback signal of AOA is sometime replaced by normal load or unused, see Fig.2, where AOA and pitch rate can be obtained from AOA sensor and angular rate gyros. Similarly side-slip angle and yaw rate are feedback for the lateral dynamics stability augmentation. So stability of the closed-loop system is enhanced by the inner loop stability augmentation control.

$$\boldsymbol{u}_{aug}^{lon} = -K_\alpha \alpha - K_q q \text{, or } \boldsymbol{u}_{aug}^{lon} = -K_q q \tag{19}$$

Now the control objective is to track a reference signal $x_{1r} = \eta_d$ with derivative $\dot{x}_{1r}$ under unknown disturbances d_ω. Thus the tracking error vectors of the attitudes are defined as

$$\begin{cases} \boldsymbol{z}_1 \triangleq \boldsymbol{x}_1 - \boldsymbol{x}_{1r} \\ \boldsymbol{z}_2 \triangleq \boldsymbol{x}_2 - \boldsymbol{x}_{2r} \end{cases} \tag{20}$$

where $\boldsymbol{x}_{1r}$ is the reference or desired trajectory and $\boldsymbol{x}_{2r}$ is the output of a command filter.

Now consider the kinematics model (3) and the dynamics model (12). The attitude controller is derived in two steps.

Step 1 (Backstepping for the variation of $\boldsymbol{z}_1$).

Consider the Lyapunov function V_1, which is required to be positive definite around the desired position as follows:

$$V_1 = \frac{1}{2} \boldsymbol{z}_1^T \boldsymbol{z}_1 . \tag{21}$$

To make the derivative function $\partial V_1 / \partial \boldsymbol{z}_1$ negative definite, a virtual control is defined as

$$\boldsymbol{\alpha}_1 = G_1^{-1} \left(\dot{\boldsymbol{x}}_{1r} - c_1 \boldsymbol{z}_1 \right) \tag{22}$$

where $G_1 = \boldsymbol{J}(\boldsymbol{\eta})$, and then

$$\frac{\partial V_1}{\partial \boldsymbol{z}_1} = \boldsymbol{z}_1^T \left(\dot{\boldsymbol{x}}_1 - \dot{\boldsymbol{x}}_{1r} \right) = \boldsymbol{z}_1^T \left(G_1 \boldsymbol{\alpha}_1 - \dot{\boldsymbol{x}}_{1r} \right) = -\boldsymbol{z}_1^T c_1 \boldsymbol{z}_1 < 0 \tag{23}$$

where $c_1 > 0$ is often chosen as a diagonal matrix to simplify the design, i.e., $c_1 = \mathrm{diag}(c_{11}, c_{12}, c_{13})$, and c_{1i} ($i = 1, 2, 3$) are positive constant.

However, instead of directly applying this virtual control $\boldsymbol{\alpha}_1$, a new signal $\boldsymbol{x}_{2r}^0$ is defined as

$$\boldsymbol{x}_{2r}^0 \triangleq \boldsymbol{\alpha}_1 - \boldsymbol{\zeta}_2 \tag{24}$$

where ζ_2 will be designed in step 2. The command signal $\boldsymbol{x}_{2r}^0$ is filtered to produce the reference signal $\boldsymbol{x}_{2r}$ and its derivative $\dot{\boldsymbol{x}}_{2r}$. It can be implemented to enforce magnitude and rate limits through this command filter. By design of the second order command filter (18), the signal $\left(\boldsymbol{x}_{2,r} - \boldsymbol{x}_{2,r}^0 \right)$ is bounded and small.

The effect of filtering on the tracking error $\boldsymbol{z}_1$ is estimated by the following stable linear filter

$$\dot{\boldsymbol{\zeta}}_1 = -c_1 \boldsymbol{\zeta}_1 + G_1 \left(\boldsymbol{x}_{2,r} - \boldsymbol{x}_{2,r}^0 \right) \tag{25}$$

where c_1 is as in (23). To remove the effect of filtering the stabilizing functions from the tracking error, the compensated tracking error is defined as

$$\tilde{z}_i \triangleq z_i - \zeta_i \, , \, (i{=}1,2) \tag{26}$$

Re-select the first Lyapunov function V_1 as a quadratic function of the compensated tracking error,

$$V_1 = \frac{1}{2} \tilde{z}_1^T \tilde{z}_1 \tag{27}$$

whose derivative is

$$\dot{V}_1 = \tilde{z}_1^T \dot{\tilde{z}}_1$$

$$= \tilde{z}_1^T \left(\dot{x}_1 - \dot{x}_{1r} - \dot{\zeta}_1 \right)$$

$$= \tilde{z}_1^T \left(G_1 x_2 - \dot{x}_{1r} - \left(-c_1 \zeta_1 + G_1 (x_{2r} - x_{2r}^0) \right) \right) \tag{28}$$

Substituting Eqs.(22) and (24) into Eq.(28) yields

$$\dot{V}_1 = \tilde{z}_1^T \left(G_1 \left(z_2 + \alpha_1 - \zeta_2 \right) \right) + \tilde{z}_1^T \left(c_1 \zeta_1 - \dot{x}_{1r} \right)$$

$$= \tilde{z}_1^T c_1 \left(\zeta_1 - \dot{x}_{1r} \right) + \tilde{z}_1^T \left(G_1 \tilde{z}_2 + \dot{x}_{1r} - c_1 z_1 \right)$$

$$= \tilde{z}_1^T G_1 \tilde{z}_2 - \tilde{z}_1^T c_1 \tilde{z}_1 \tag{29}$$

Now a SMC control is introduced to improve system adaptiveness, the sliding surface s is designed as

$$s = \lambda_1 \tilde{z}_1 + \tilde{z}_2 \quad , \tag{30}$$

where λ_1 is the control gains to be determined.

The well-known characteristics of SMC are attraction and invariance, which means the condition for the state to reach the sliding mode surface s in finite time t_r and remain it, i.e.,

$$s\dot{s} < 0, \quad t < t_r \tag{31}$$

$$s = \dot{s} = 0, \ t \geq t_r \tag{32}$$

For the sliding mode surface of Eq.(30), the reachability condition is designed as

$$\dot{s} = -\hbar s - \varsigma \operatorname{sgn}(s), \tag{33}$$

so their corresponding attraction and invariance for the SMC are as follows

$$s\dot{s} = -\hbar s^T s - \varsigma |s| \tag{34}$$

where $\hbar$, and ς are sliding mode surface parameters with $\hbar > 0$, and $\varsigma > 0$.

Step 2 (Calculate the INBSM control)

The effect of filtering the command signal on the tracking error $\mathbf{z}_2$ is estimated by the following stable linear filter

$$\dot{\boldsymbol{\zeta}}_2 = -c_2 \boldsymbol{\zeta}_2 + G_2 \left(\boldsymbol{u}_{INBS} - \boldsymbol{u}_{INBS}^0 \right) \tag{35}$$

where G_2 is as in (5), c_2 is the filter gain to be determined, $\boldsymbol{u}_{INBS}^0$ is the incremental backstepping sliding mode control to be designed, and $\boldsymbol{u}_{INBS}$ is the filtered output of $\boldsymbol{u}_{INBS}^0$.

Now consider that the unobservable disturbance of d_ω, it can be approximated by the neural network. Construct the second candidate Lyapunov function as

$$V_2 = V_1 + \frac{1}{2} s^T s + \frac{1}{2} (1/\gamma_W) \tilde{W}^T \tilde{W}, \tag{36}$$

where $\tilde{W}$ is estimation error of the weight function W meeting $\tilde{W} = W^* - \hat{W}$, γ_w is a positive constant that determines the convergence speed of the NN approximation. Differentiating (36) yields

$$\dot{V}_2 = -\tilde{z}_1^T c_1 \tilde{z}_1 + \tilde{z}_1^T G_1 \tilde{z}_2 + s^T \dot{s} + (1/\gamma_W) \tilde{W}^T \dot{\tilde{W}} \quad . \tag{37}$$

Substituting (20), (23),(29), (35) into (37) yields

$$\dot{V}_2 = -\tilde{z}_1^T c_1 \tilde{z}_1 + \tilde{z}_1^T G_1 \tilde{z}_2 + s^T \dot{s} - (1/\gamma_W) \tilde{W}^T \dot{\hat{W}}$$

$$= -\tilde{z}_1^T c_1 \tilde{z}_1 + \tilde{z}_1^T G_1 \tilde{z}_2 + s^T \left(\lambda_1 \dot{\tilde{z}}_1 + \dot{\tilde{z}}_2 \right) - (1/\gamma_W) \tilde{W}^T \dot{\hat{W}}$$

$$= -\tilde{z}_1^T c_1 \tilde{z}_1 + \tilde{z}_1^T G_1 \tilde{z}_2 + s^T \left(\lambda_1 \left(c_1 \tilde{z}_1 + G_1^T \tilde{z}_2 \right) + \left(f_2 + G_2 u_{INBS} + g_{d_\omega} d_\omega - \dot{x}_{2r} + c_2 \zeta_2 - G_2 \left(u_{INBS} - u_{INBS}^0 \right) \right) \right) - (1/\gamma_W) \tilde{W}^T \dot{\hat{W}}$$

$$= -\tilde{z}_1^T c_1 \tilde{z}_1 + \tilde{z}_1^T G_1 \tilde{z}_2 + s^T \left(\lambda_1 \left(c_1 \tilde{z}_1 + G_1^T \tilde{z}_2 \right) + f_2 + G_2 u_{INBS}^0 + W^{*T} h + \varepsilon - \dot{x}_{2r} + c_2 (z_2 - \tilde{z}_2) \right) - (1/\gamma_W) \tilde{W}^T \dot{\hat{W}} \quad (38)$$

By using the sliding surface (30) and reaching law (33), a desired control input (in non-incremental form) is designed as follows to make (38) semi-negative definite,

$$u_{INBS}^0 = G_2^{-1} \left(-\lambda_1 \left(c_1 \tilde{z}_1 + G_1^T \tilde{z}_2 \right) - c_2 (z_2 - \tilde{z}_2) - G_1^T \tilde{z}_1 - f_2 + \dot{x}_{2r} - \hat{W}^T h - \left(\hbar s + \varsigma \, \mathrm{sgn}(s) \right) \right), \quad (39)$$

Since

$$s^T \tilde{d}_\omega = \tilde{d}_\omega^T s, \quad \tilde{z}_1^T G_1 \tilde{z}_2 = \tilde{z}_2^T G_1^T \tilde{z}_1 \quad (40)$$

Substituting (39) and (40) into (38) yields

$$\dot{V}_2 = \left(-\tilde{z}_1^T c_1 \tilde{z}_1 + \tilde{z}_1^T G_1 \tilde{z}_2 \right) - \hbar s^T s - \varsigma \, | \, s \, | + s^T \left(\tilde{W}^T h + \varepsilon \right) - (1/\gamma_W) \tilde{W}^T \dot{\hat{W}} \quad (41)$$

Choose the update law of the NN weight function as:

$$\dot{\hat{W}} = \gamma_W s^T h(x) \quad (42)$$

and substitute (42) into (41) yields

$$\dot{V}_2 = \left(-\tilde{z}_1^T c_1 \tilde{z}_1 + \tilde{z}_1^T G_1 \tilde{z}_2 \right) - \hbar s^T s - \varsigma \, | \, s \, | + s^T \varepsilon \quad (43)$$

Define Q as a positive definite symmetric matrix

$$Q \triangleq \begin{bmatrix} c_1 + \hbar \lambda_1^2 & \lambda_1 \hbar - \dfrac{1}{2} G_1 \\ \lambda_1 \hbar - 0.5 G_1 & \hbar I_n \end{bmatrix} \quad (44)$$

where I_n denotes the $n \times n$ unit matrix. Let $Z_{12} \triangleq \begin{bmatrix} \tilde{z}_1^T & \tilde{z}_2^T \end{bmatrix}^T$, this then yields

$$Z_{12}^T Q Z_{12} = \tilde{z}_1^T c_1 \tilde{z}_1 + \hbar \lambda_1^2 \tilde{z}_1^T \tilde{z}_1 + 2\lambda_1 \hbar \tilde{z}_1^T \tilde{z}_2 - \tilde{z}_1^T G_1 \tilde{z}_2 + \hbar \tilde{z}_2^T \tilde{z}_2$$

$$= \tilde{z}_1^T c_1 \tilde{z}_1 - \tilde{z}_1^T G_1 \tilde{z}_2 + \hbar \left(\lambda_1 \tilde{z}_1 + \tilde{z}_2 \right)^T \left(\lambda_1 \tilde{z}_1 + \tilde{z}_2 \right)$$

$$= \left(\tilde{z}_1^T c_1 \tilde{z}_1 - \tilde{z}_1^T G_1 \tilde{z}_2 \right) + \hbar s^T s \quad .$$

$$\quad (45)$$

Substituting (45) into (43) yields

$$\dot{V}_2 = -Z_{12}^T Q Z_{12} - \varsigma \, | \, s \, | + s^T \varepsilon \quad .$$

(46)

Using (44), it is obtained that

$$|Q| = \left\| \begin{matrix} c_1 + \hbar\lambda_1^2 & \lambda_1\hbar - 0.5G_1 \\ \lambda_1\hbar - 0.5G_1 & \hbar I_n \end{matrix} \right\|$$

$$= \hbar(c_1 + \lambda_1 G_1) - G_1^T G_1 / 4 . \tag{47}$$

If the following condition is satisfied,

$$\hbar(c_1 + \lambda_1 G_1) > G_1^T G_1 / 4 , \tag{48}$$

then Q is positive definite. Since $|\varepsilon| \le \bar{\varepsilon}$ (from Eq.(14)),then $s^T \varepsilon \le |s^T| \cdot |\varepsilon| < \bar{\varepsilon} |s^T|$, and if $\varsigma > \bar{\varepsilon} > 0$, then

we have

$$\left(-\varsigma + \bar{\varepsilon}\right)|s| = -\varsigma|s| + \bar{\varepsilon}|s^T| < 0 , \tag{49}$$

and then $-\varsigma|s| + s^T \varepsilon < 0$. So

$$\dot{V}_2 = -Z_{12}^T Q Z_{12} - \varsigma|s| + s^T \varepsilon < 0 . \tag{50}$$

Therefore, the closed-loop system is stable by Lyapunov theory.

Remark 3 In order to effectively eliminate the chattering phenomenon of reachability condition (33)

in the sliding mode control, a continuous function is used to define practical sliding surface dynamics

using a "tanh" function,

$$\dot{s} = -\hbar s - \varsigma \tanh(s / \phi) , \tag{51}$$

where ϕ is sliding surface boundary layer parameters used to retain continuity of control as motion

trajectories cross the sliding surface and prevent chattering. High frequency chattering of the control is

prevented by using the boundary layer.

3.3 Incremental nonlinear backstepping attitude tracking control

It can clear that NDI control law depends on accurate knowledge of the aerodynamic model

contained in both M_a and M_c, and depends on the model uncertainties and disturbances; if the

disturbance information is unknown, it does not reject the disturbances. So an incremental

backstepping control design is proposed to achieve a more flexible and augmented design. According

to Fig.2, the composite controller input of the tracking system is

$$\boldsymbol{u}_c \triangleq \boldsymbol{u}_{INBSM0} + \boldsymbol{u}_{aug} + \boldsymbol{u}_d + \boldsymbol{u}_f \tag{52}$$

where $\boldsymbol{u}_d$ are $\boldsymbol{u}_f$ are compensation control inputs of disturbances and faults, respectively,

$\boldsymbol{u}_{INBSM0} = \delta_0 + \boldsymbol{u}_{INBSM}$.

To obtain an incremental Backstepping control $\boldsymbol{u}_{INBSM}$, for simplicity, we start from **Step 2** of the

backstepping design procedure in Section 3.2, assuming that the outer subsystem's stabilizing control

law are already obtained and stepped back up to the dynamic equation in consider.

For the BWB aircraft, the model (12) of the attitude dynamics can be represented as follows

$$\overline{\boldsymbol{I}}\dot{\omega} = \left(-\omega \times \left(\overline{\boldsymbol{I}}\omega\right) + \boldsymbol{M}_a\right) + \left(\boldsymbol{M}_c\right)_\delta \delta + g_{d_\omega} d_\omega \tag{53}$$

where $\boldsymbol{M}_a = \overline{q}S\begin{bmatrix} bC_{la} & \overline{c}C_{ma} & bC_{na}\end{bmatrix}^T, \delta = \begin{bmatrix} \delta_a & \delta_e & \delta_r \end{bmatrix}^T, \left(\boldsymbol{M}_c\right)_\delta$ is as in (5).

Now we depart from the error dynamics equation by using Eqs (24) and (26),

$$\dot{\overline{z}}_2 = \dot{\boldsymbol{x}}_2 - \dot{\boldsymbol{x}}_{2r} - \dot{\boldsymbol{\zeta}}_2 = \dot{\boldsymbol{x}}_2 - \dot{\overline{\alpha}}_1(\sigma,\omega) \tag{54}$$

that is,

$$\dot{\overline{z}}_2 = \dot{\omega} - \dot{\overline{\alpha}}_1(\sigma,\omega) = \boldsymbol{f}_2(x) + G_2(x)\delta + g_{d_\omega} d_\omega - \dot{\overline{\alpha}}_1(\sigma,\omega) \tag{55}$$

where σ may represent a kinematics variable or a state stepped back from the outer subsystems,

$\dot{\overline{\alpha}}_1(\sigma,\omega) = \dot{\alpha}_1(\sigma,\omega) + G_1^{-1}\left(\ddot{\zeta}_1 + c_1\dot{\zeta}_1\right)$, according to the filter (18), the signal $\left(\boldsymbol{x}_{2,r} - \boldsymbol{x}_{2,r}^0\right)$ is bounded

and small, so $\dot{\overline{\alpha}}_1$ can be approximated by $\dot{\alpha}_1$. As $\boldsymbol{f}_2(x) = \overline{\boldsymbol{I}}^{-1}\left(\boldsymbol{M}_a - \omega \times \left(\overline{\boldsymbol{I}}\omega\right)\right), G_2 = \overline{\boldsymbol{I}}^{-1}\left(\boldsymbol{M}_c\right)_\delta$, for

flight control law design, the goal is to stabilize the complete system described by the following

augmented equation

$$\dot{\overline{z}}_2 = \overline{\boldsymbol{I}}^{-1}\left(\boldsymbol{M}_a - \omega \times \left(\overline{\boldsymbol{I}}\omega\right)\right) + \overline{\boldsymbol{I}}^{-1}\left(\boldsymbol{M}_c\right)_\delta \delta + \overline{\boldsymbol{I}}^{-1}g_{d_\omega} d_\omega - \dot{\overline{\alpha}}_1(\sigma,\omega) \tag{56}$$

Applying backstepping to Eq.(55), the actuator input of the BWB aircraft is

$$\delta = \left(M_c \right)_\delta^{-1} \overline{I} \left[-K_\omega \tilde{z}_2 - \overline{I}^{-1} \left(M_a - \omega \times \left(\overline{I} \omega \right) \right) + \dot{\overline{\alpha}}_1(\sigma, \omega) + \Gamma_d \right] \tag{57}$$

where the control gain is $K_\omega > 0$ and the damping term is $\Gamma_d = -\overline{I}^{-1} \hat{W}^T h$, which is used to reject the unobservable disturbances and model uncertainty. The robustness of such a backstepping design is improved by introducing its incremental counterpart, using the implicit approach with the recursive control law

$$\delta = \delta_0 + \left(M_c \right)_\delta^{-1} \overline{I} \left[-K_\omega \tilde{z}_2 - \dot{\omega}_0 + \dot{\overline{\alpha}}_1(\sigma, \omega) + \Gamma_d \right] \tag{58}$$

According to the backstepping control law (39) and considering the approximate dynamics around the current reference state for the dynamics $\dot{\omega} \approx \dot{\omega}_0 + G_2 \Delta\delta$, the backstepping control (39) can be rewritten in incremental form,

$$\Delta\delta = G_2^{-1} \left(-\lambda_1 \left(c_1 \tilde{z}_1 + G_1^T \tilde{z}_2 \right) - c_2 (z_2 - \tilde{z}_2) - G_1^T \tilde{z}_1 - \dot{\omega}_0 + \dot{x}_{2r} - \hat{W}^T h - \left(\hbar s + \varsigma \, \mathrm{sgn}(s) \right) \right). \tag{59}$$

The output $\dot{\omega}_0$ represents the current estimated angular acceleration, which is measured by differentiating the angular rates. The approximation function from the ω_0 to derivative $\dot{\omega}_0$ is

$$H_\omega(s) = \frac{s\omega_n^2}{s^2 + 2\zeta\omega_n s + \omega_n^2} \, . \tag{60}$$

Theorem 3.1 There exists a composite controller of u_{INBSM} and u_d with a disturbance observer of (8) that guarantees the closed-loop system of (7) meeting desired performances of (a) and (b), if the positive-definition control gain of K_ω meets Eq.(57), the observer gain $l(x)$ is appropriately determined such that all the eigenvalues of matrix $-l(x)g_{d_\omega}$ have negative real part, and the positive-definition filter gain matrices of c_1 and c_2 meet Eqs (25) and (35), the sliding mode control (30) and (34) satisfy that Q and λ_1 is positive definite, and $\hbar > 0$, $\varsigma > \overline{\varepsilon} > 0$, and update law of the NN weight function of (42) meets $\gamma_W > 0$.

Proof.

If there exist a positive-definition control gains of K_ω meets Eqs.(57) and (59), then the control input of the INBSM controller $\boldsymbol{u}_{INBSM0}$ is obtained, so the INBSM controller of (57) and (59) can meet Eq.(39), which guarantees the candidate Lyapunov function $V_2 > 0$, $\dot{V}_2 < 0$, yield the result. ∎

Remark 4 It suffices to consider the new $f_2 = \dot{x}_{2_0} = \dot{\omega}_0$, noticing that we are replacing the accurate knowledge of f_2 by a measurement (or an estimate) instead [21], and this trade-off results in a robustified backstepping control law which is not entirely dependent on the model. Comparing with Eq.(57), there does not exist an $\dot{\alpha}_1$ term for (58), so it can be directly obtained.

For the BWB aircraft, the elevator, aileron, rudder and engine actuator dynamics can be simplified as 1st order models,

$$G_{\delta_i}(s) = \frac{T_{\delta_i}}{s + T_{\delta_i}} \tag{61}$$

where $\delta_i = \delta_a, \delta_e, \delta_r, \delta_p$ T_{δ_i} are the actuator time constants.

Finally, consider fault of the system Eq.(17), two faults of actuator bias and loss of effectiveness are considered, and then the fault model of (16) can be rewritten as

$$\boldsymbol{u}_a(t) = \bar{\rho}_a \boldsymbol{u}(t) + \boldsymbol{u}_f \tag{62}$$

where $\boldsymbol{u}_f = \left(\boldsymbol{I} - \bar{\rho}_a\right) \boldsymbol{f}_a$.

Theorem 3.2 There exists a composite controller of (52) with a disturbance observer (8) and a fault estimator (65) that guarantees the closed-loop system (7) meets desired performances of (a) and (b), if the positive-definition control gain of K_ω meets Eq.(57), the observer gain $l(x)$ is appropriately determined such that all the eigenvalues of matrix $-l(x)g_{d_\omega}$ have negative real part, and the positive-definition filter gain matrices of c_1 and c_2 meet Eqs (25) and (35), the sliding mode control (30) and (34) satisfy that Q and λ_1 is positive definite, and $\hbar > 0$, $\varsigma > \bar{\varepsilon} > 0$, and update law of the NN weight function of (42) meets $\gamma_W > 0$, positive definite weight matrix $\boldsymbol{P}_f$ and γ_f make Eq.(65) be

convergent.

Proof

Based on **Theorem 3.1**, the second augmented closed-loop Lyapunov function of (29) is changed for backstepping as follows when actuator faults occur

$$V_2 = V_1 + \frac{1}{2}s^T s + \frac{1}{2}(1/\gamma_W)\tilde{W}^T\tilde{W} + \frac{1}{2\gamma_d}\tilde{u}_f^T P_f^{-1}\tilde{u}_f \tag{63}$$

where $\tilde{u}_f = \hat{u}_f - u_f$ is the fault estimation error, and P_f is a positive definite weight matrix.

Substituting (50) into the following derivative of V_2 yields

$$\dot{V}_2 = -Z_{12}^T Q Z_{12} - \varsigma\,|\,s\,| + s^T\varepsilon + \tilde{u}_f^T P_f^{-1}\dot{\tilde{u}}_f \tag{64}$$

The fault estimator is designed as:

$$\dot{\hat{u}}_f = P_f G_2^T \tilde{z}_2 - \gamma_f \hat{u}_f \tag{65}$$

which yields

$$\tilde{u}_f^T P_f^{-1}\dot{\tilde{u}}_f = \tilde{u}_f^T P_f^{-1}\left(\dot{\hat{u}}_f - \dot{u}_f\right) = \tilde{u}_f^T P_f^{-1} P_f G_2^T \tilde{z}_2 - \tilde{u}_f^T P_f^{-1}\gamma_f \hat{u}_f - \tilde{u}_f^T P_f^{-1}\dot{u}_f$$

$$= \tilde{u}_f^T G_2^T \tilde{z}_2 - P_f^{-1}\gamma_f \tilde{u}_f^T \hat{u}_f - P_f^{-1}\tilde{u}_f^T \dot{u}_f \tag{66}$$

Since $\|\,u_f\,\| \le \|\bar{u}_{\max}\| < \infty, \|\,\dot{u}_f\,\| \le \|\bar{\dot{u}}_{\max}\| < \infty$, $\bar{u}_{\max}$ and $\bar{\dot{u}}_{\max}$ denote upper bounds of the actuator position and rotating rate, then [33]

$$-P_f^{-1}\gamma_f \tilde{u}_f^T \hat{u}_f = -P_f^{-1}\gamma_f \tilde{u}_f^T\left(\tilde{u}_f + u_f\right)$$

$$\le \frac{1}{2}\left(-P_f^{-1}\gamma_f \tilde{u}_f^T \tilde{u}_f + P_f^{-1}\gamma_f \bar{u}_{\max}^T \bar{u}_{\max}\right) \tag{67}$$

$$-P_f^{-1}\tilde{u}_f^T \dot{u}_f \le \frac{1}{2}\left(P_f^{-1}\tilde{u}_f^T\tilde{u}_f + P_f^{-1}\bar{\dot{u}}^T\bar{\dot{u}}\right) \le \frac{1}{2}\left(P_f^{-1}\tilde{u}_f^T\tilde{u}_f + P_f^{-1}\bar{\dot{u}}_{\max}^T\bar{\dot{u}}_{\max}\right) \tag{68}$$

Substitute (67), (68) into (66) yields

$$\tilde{u}_f^T P_f^{-1}\dot{\tilde{u}}_f \le \tilde{u}_f^T G_2^T \tilde{z}_2 + \bar{c} \tag{69}$$

where $P_f = diag(1,1,1)$, $\gamma_f = diag(1,1,1)$

$$\overline{c} = \frac{\gamma_f}{2P_f}\left(-\tilde{u}_f^T\tilde{u}_f + \overline{u}_{max}^T\overline{u}_{max}\right) + \frac{1}{2P_f}\left(\tilde{u}_f^T\tilde{u}_f + \overline{u}_{max}^T\tilde{u}_{max}\right). \tag{70}$$

As fault estimation error $\tilde{u}_f$ is a small variant for the fault estimator (65) [33], thus finally yields

$$\dot{V}_2 = -Z_{12}^T Q Z_{12} - \varsigma|s| + s^T\varepsilon + \overline{c} \tag{71}$$

Let $c_k = \min\{2|Q|, -\gamma_f+1\}$, and if $\varsigma > \overline{\varepsilon} > 0$, then

$$\dot{V}_2 \le -c_k V_2 + \overline{c} \tag{72}$$

According to LaSalle-Yoshizawa Lemma [34] and reference [33], the closed-loop system tracking error will exponentially converge, and

$$V_2 \le \left(V_2(0) - \overline{c}/c_k\right)e^{-c_k t} + \overline{c}/c_k \tag{73}$$

Hence

$$\frac{1}{2}Z_{12}^T Z_{12} \le V_2, \|Z_{12}\| \le \sqrt{\frac{2\overline{c}}{c_k}}, \tag{74}$$

that is, the desired tracking error will exponentially converge to the set

$$\|\tilde{z}_1\| + \|\tilde{z}_2\| \le \sqrt{\frac{2\overline{c}}{c_k}}, \tag{75}$$

and

$$\|x_1\| = \|\tilde{z}_1 + \zeta_1\| \le \|\tilde{z}_1\| + \|\zeta_1\|, \|x_2\| = \|\tilde{z}_2 + \zeta_2\| \le \|\tilde{z}_2\| + \|\zeta_2\|. \qquad \blacksquare \tag{76}$$

According to Fig.2, the algorithm flow chart of the proposed NNDO-INBSM control is as follows,

Step 1 Calculate error signals

$$\left.\begin{array}{l}\eta,\omega\\x_{1r},x_{2r}\end{array}\right\}\xrightarrow{Eq.(20)}\begin{pmatrix}z_1\\z_2\end{pmatrix};\quad\left.\begin{array}{l}z_1,z_2\\\dot{x}_{1r},\eta\end{array}\right\}\xrightarrow{Eq.(22)}\alpha_1;\quad\left.\begin{array}{l}\eta,x_{2r}^0,x_{2r}\\u_{INBS}^0,u_{INBS}\end{array}\right\}\xrightarrow{Eqs(25),(35)}\begin{pmatrix}\zeta_1\\\zeta_2\end{pmatrix};$$

$$\left.\begin{array}{l}z_1,z_2\\\zeta_1,\zeta_2\end{array}\right\}\xrightarrow{Eq.(26)}\begin{pmatrix}\tilde{z}_1\\\tilde{z}_2\end{pmatrix};\quad\left.\begin{array}{l}\tilde{z}_1\\\tilde{z}_2\end{array}\right\}\xrightarrow{Eq.(30)}s;$$

Step 2 Calculate NNDO and disturbance estimation $\hat{D}_\omega$ by Eqs (8), (11), and (14);

Step 3 Calculate the augmentation control u_{aug} by Eq.(19)

Step 4 Calculate the incremental BSMC control $\boldsymbol{u}_{INBS}$ with NNs compensation by Eq.(59).

Step 5 Calculate the fault estimation $\hat{\boldsymbol{u}}_f$ by Eq.(65)

Step 6 Calculate the total control input u_c by Eq.(52)

Step 7 repeat step1 to step6 until all tracking tasks are complemented.

4. **Simulation and analysis**

The considered model is a 50.8m length, 80m wing span BWB aircraft [7, 8], the aerodynamics

coefficient parameters are as in Ref.[7], and the structure parameters of the BWB aircraft are listed in

Table 1.

Table 1 Parameters for the studied BWB aircraft

Parameter	Value	Unit	Coefficient	Value	Unit
m	3.7×10^5	kg	$T_{\delta a}$	15	sec
S	841.7	m^2	$T_{\delta e}$	15	sec
$\overline{c}$	12.31	m	$T_{\delta r}$	15	sec
b	80	m	$T_{\delta p}$	1	sec
x_G,	30.4	m	z_G	0	m
I_{xx}	4.703×10^7	kg·m^2	I_{yy}	2.507×10^7	kg·m^2
I_{zz}	9.973×10^7	kg·m^2	I_{xz}	0.0	kg·m^2

The aircraft flight is at 20000ft (6096m) altitude and 375kts (191.9m/s) speed, the trim state

$$x_e = \begin{bmatrix} u & w & q & \theta & h & x & v & p & r & \phi & \psi & y \end{bmatrix}_e^T,$$

$= [191.92\ 18.31\ 1.31\ 0.095\ 6096\ 1.18e-16\ 2.52e-20\ -1.40e-25\ -1.09e-25\ 5.93e-23\ 0\ 0]^T$, unit: [u v

w] (m/s), [p q r] (rad/s), [x y h] (m), [φ,θ,ψ](rad).

$$u_e = \begin{bmatrix} \delta_e & \delta_p & \delta_a & \delta_r \end{bmatrix}_e^T = [-0.11\ 0.33\ 5.59e-22\ 1.28e-21]^T, \quad \text{unit: } [\delta_a\ \delta_e\ \delta_r]\ (rad).$$

The position range for the actuators are $\delta_e \in [-0.35, 0.26]$ (rad), $\delta_p \in [0, 1]$, $\delta_a \in [-0.65, 0.65]$ (rad), δ_r

$\in [-0.38, 0.38]$ (rad). The initial position is set to $\xi_0 = [0, 0, -6096m]^T$, with initial body velocity $V_0 =$

[192 m/s, 0, 0]^T, initial attitude $\eta_0 = [0, 5.5°, 0]^T$, and initial angular velocity $\omega_0 = [0, 0, 0]^T$. For the

command filter (18), the damping ratio is selected as $\zeta_n = 0.9$, and natural frequency is selected as $\omega_n = 10$ rad/s to avoid large maneuver inputs.

Scenario I: Stability augmentation control with different center of gravity

According to stability requirement of the BWB aircraft [7, 8], center of gravity (CG) can move along the longitudinal axis in the range of 29.4m ~34.4m, see Fig.1. To illustrate the proposed method in stability augmentation, the controller parameters are designed as follows:

$$c_1 = \text{diag}([0.1, 0.3, 0.3]), \quad c_2 = \text{diag}([1\ 1/3\ 0.4]), \tag{77}$$

and the augment stability control gains

$$K_\alpha = 0.01, \quad K_q = 0.3,$$

the RBF NN parameters are set as

$\gamma_W = 10$, $c = [-1\ 0\ 1; -1\ 0\ 1; -1\ 0\ 1; -1\ 0\ 1; -1\ 0\ 1; -1\ 0\ 1]$; $b_j = 0.002$; $h(0) = [0.01, 0.01, 0.01]^T$;

the siding mode control parameters are designed as

$$\lambda_1 = 0.1 * \text{diag}([1, 1, 1]), \hbar = 0.1 * \text{diag}([1, 1, 1]), \varsigma = \text{diag}([1.0\ 1.2\ 1.0]), \quad \phi = 0.4,$$

where c_1 and c_2 are in Eq.(25) and Eq.(35), K_α and K_β are selected to satisfy the requirements in Section 3 after several design iterations. A doublet command is predefined as the desired attitude to verify the tracking performance of the NNDO-INBSM. An INDI proposed by Lu and Kampen [19] is used to compare the proposed controller performances, where control gains are designed as

$$K_\eta = \text{diag}([0.4\ 0.4\ 0.4]), \quad K_\omega = \text{diag}([22.5\ 45\ 1.125]), \tag{78}$$

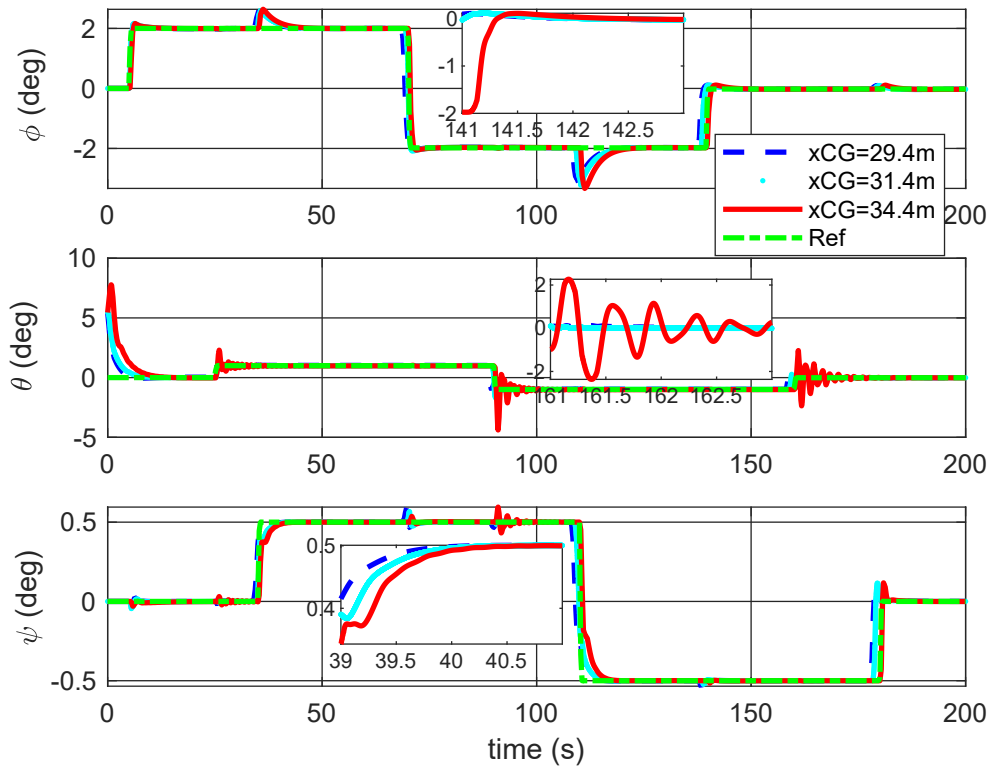The simulation results are shown in Figs 3-6.

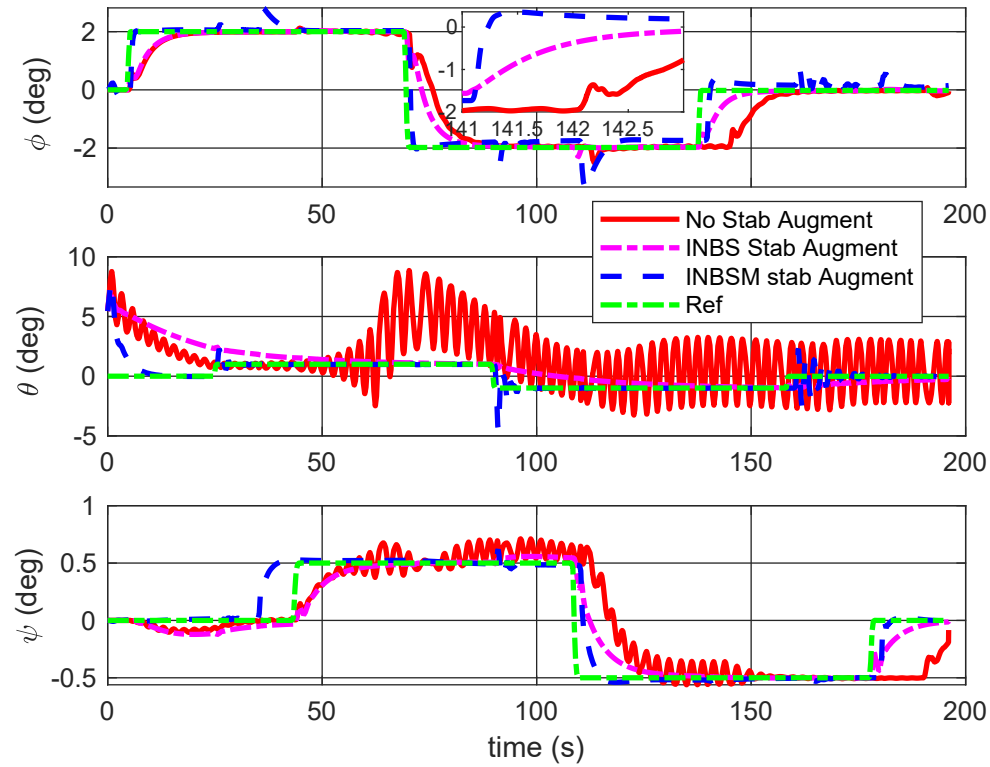Fig.3. Stability augmentation responses by INBSM control under different CG positions

Fig.4. Stability augmentation control responses

From Figs 3 and 4, it can be seen that the responses of the forward CG position converge faster than those of the aftward CG position. When the CG position move backwards to x_{CG} = 34.4m, which is outside the range of the limitation, see Fig.1, the responses of pitch and yaw motion begin to oscillate and become unstable without augmentation control, see Fig.4. When the stability augmentation control is added, the tracking responses for the Euler angles are stable and converge to steady values, this is because the stability augmentation improves the system damping rate and frequency of pitch motion. Meanwhile, the tracking responses by using INBSM design are faster than those by using INBS control, this shows the sliding mode control has better adaptive capability. The control inputs of the INBSM design are shown in Fig.5.
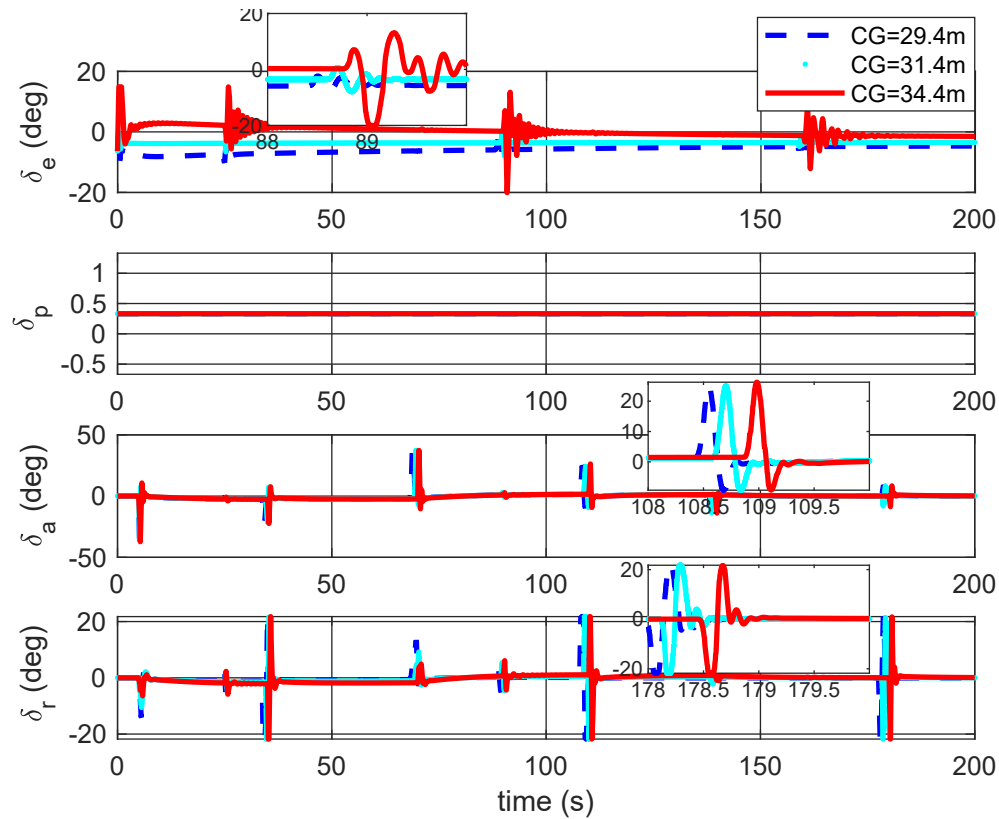
Fig.5. Control inputs of INBSM control under different CG positions

From Fig.5 it can be seen that the further back the CG position, the bigger the elevator inputs. This is because the more aftward the CG position, the more the aircraft is unstable, and it needs more elevator

input to balance pitch moment of aerodynamic forces, where the pitch moment arm of $|x_{AC} - x_{CG}|$ is bigger (AC denotes aerodynamic center).

Scenario II: Attitude tracking control

Case 1: Unknown disturbances inputs.

In this scenario suppose that there is the unknown disturbance vector D_ω acting on the BWB aircraft, given by

$$D_\omega(t) = \bar{I} \times [0.025 \ -0.025 \ 0.015]^T. \tag{79}$$

The gains of the disturbance observer (8) are designed as

$$l(x) = \text{diag}([.25, .00022, .0105]). \tag{80}$$

To illustrate the proposed method in attitude control, an INBS control proposed by Acquatella [21] and an adaptive fuzzy control referred as in Ref.[35]- Ref.[37] are used to compare, and the controller parameters of the INBS control are designed as Scenario I. For the adaptive fuzzy control, the fuzzy sets are defined as NL, NS, ZO, PS, and PL, which denote negative large, negative small, zero, positive small, positive large, and their center points are selected as $-\dfrac{\pi}{6}, \ -\dfrac{\pi}{12}, \ 0, \ \dfrac{\pi}{12}, \ \dfrac{\pi}{6},$ respectively. The fuzzy membership functions are chosen as

$$\mu_{Fi,j}(x) = \exp\left[-\left(\left(x_j + \frac{\pi}{6} - (i-1)\cdot\frac{\pi}{12}\right)\middle/\frac{\pi}{24}\right)^2\right] (i = 1,2,\ldots,5, j = 1,2,\ldots,n), \tag{81}$$

Assume function $f_2(x), g_2(x)$ are unknown, The following fuzzy logic systems are used to approximate them,

$$\hat{f}_2(\hat{x}\,|\,\hat{\theta}_f) = \hat{\theta}_f^T \xi(\hat{x}), \quad \hat{g}_2(\hat{x}\,|\,\hat{\theta}_g) = \hat{\theta}_g^T \zeta(\hat{x}), \tag{82}$$

where $\hat{x}$ is the estimation of the state x, that is, $x^T = \begin{bmatrix} \eta^T & \omega^T \end{bmatrix}$. The fuzzy basis functions

$$\xi_i(x) = \frac{\Pi_j^n \mu_{i,j}(x_j)}{\sum\limits_{i=1}^{N}\left(\Pi_j^n \mu_{i,j}(x_j)\right)}, \tag{83}$$

$$\hat{f}_2(x_d\,|\,\hat{\theta}_f) = \hat{\theta}_f^T \xi(x_d), \quad \hat{g}_2(x_d\,|\,\hat{\theta}_g) = \hat{\theta}_g^T \zeta(x_d). \tag{84}$$

For each channel of roll, pitch and yaw, select the vector $K = \begin{bmatrix} k_2 \\ k_1 \end{bmatrix} = \begin{bmatrix} 2 \\ 1 \end{bmatrix}$, such that the following

equation holds $A^T P + PA = -Q$, where $A = \begin{bmatrix} 0 & -k_2 \\ 1 & -k_1 \end{bmatrix}$, $Q = \begin{bmatrix} 10 & 0 \\ 0 & 10 \end{bmatrix}$, P is a symmetric positive

definite matrix. The adaptive laws are $\dot{\theta}_f = -\gamma_1 e^T Pb\xi(x)$, $\dot{\theta}_g = -\gamma_2 e^T Pb\zeta(x)u$, $e = x_d - x$, $\gamma_1 = 10$,

$\gamma_2 = 1$, b= $[0\ 1]^T$, the fuzzy control output $u_F = \dfrac{1}{\hat{g}_2}\left(-\hat{f}_2 + K^T e + \ddot{x}_{1r}\right)$ as the input of the inner loop of

angular rate for nonlinear dynamic inversion control, so the adaptive fuzzy control for the outer loop

of attitudes with a nonlinear dynamic inversion control for the inner loop of angular rate is

implemented. The parameters of the nonlinear dynamic inversion control are the same as Eq.(78). The

simulation results are shown in Figs 6-8.
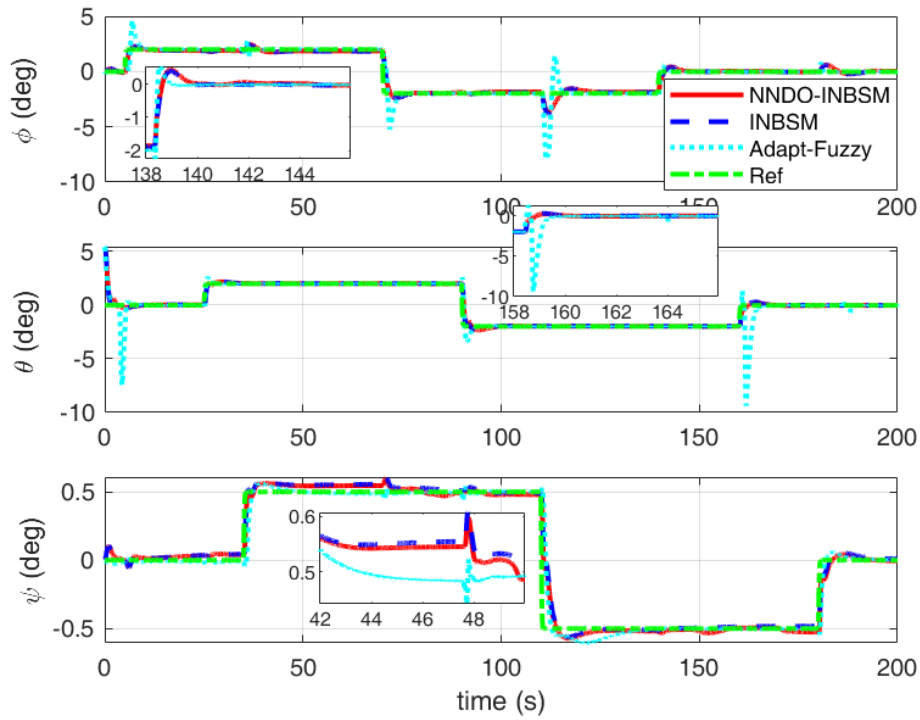
Fig.6. Attitude tracking responses under unknown disturbances

From Fig.6, it can be seen that the three methods can track the desired attitudes, but the adaptive fuzzy

control responses have larger overshoots and errors than those of the INBS and NNDO-INBSM design,

this is because adaptive fuzzy control requires more control inputs. Meanwhile, there are larger

overshoots of INBSM control than those of NNDO-INBSM control in pitch, roll and yaw motions, this

shows NNDO-INBSM can compensate for the observable disturbances or input changes and make their

responses smooth. The disturbances have been observed via disturbance observers as shown in Figs 7
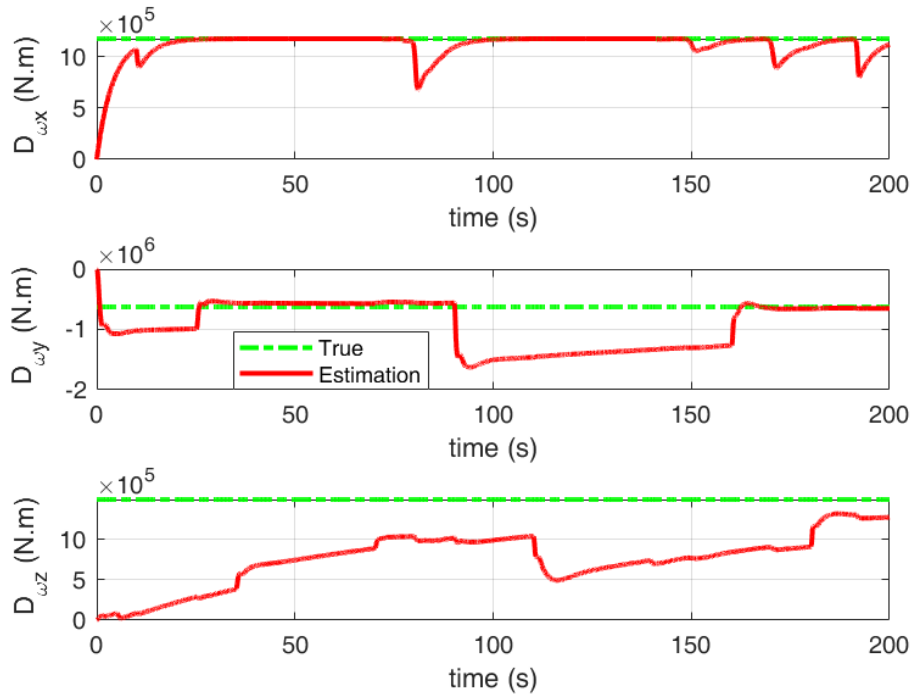
and 8.

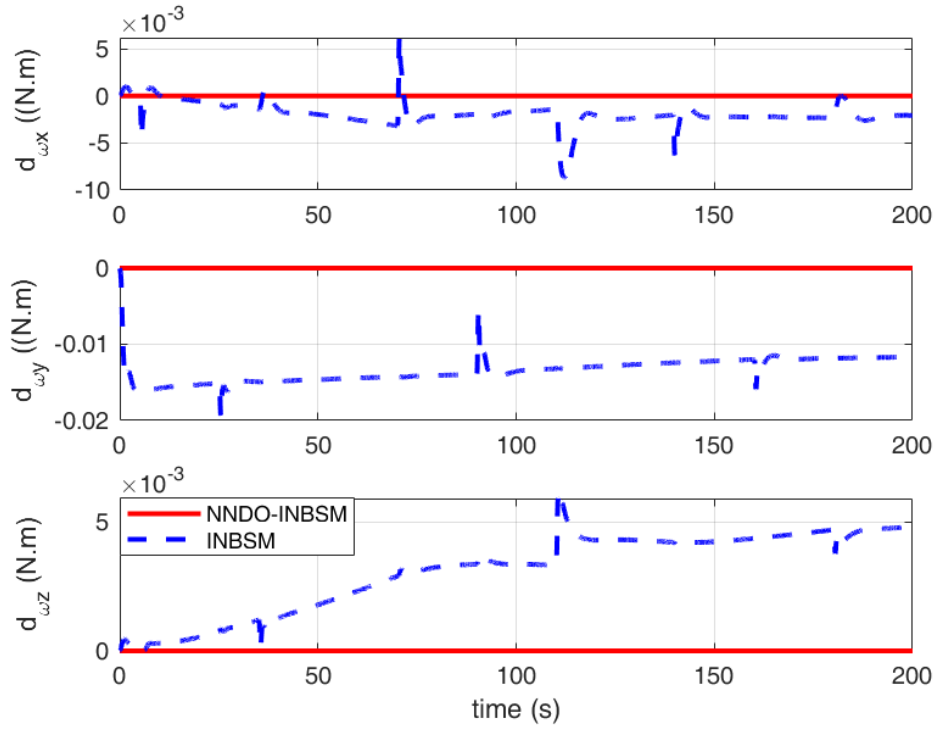Fig.7. Observable disturbance estimation

Fig.8. Unobservable disturbance approximation

From Fig.7 it can be seen that roll moment disturbance can be precisely estimated, but yaw and pitch moments have some errors during transition due to the disturbance estimation varying with the associated states, as $p(x) = l(x) x$ in Remark 1, and their steady values converge to the true ones. Fig.8 shows that there are large steady errors of INBSM compared with those of NNDO-INBSM, which demonstrates that NNDO-INBSM can reduce the observable disturbances.

Case 2: Model parameter uncertainties with unknown disturbances

This scenario considers model parameter uncertainty due to aerodynamic derivatives varying accordingly with angle of attack (AOA) and side-slip angle. Hence the aerodynamic coefficients C_x are set with 20% uncertainties $\Delta C = 0.2 C_x$, where $\triangle$ denotes the perturbation value. Here the parameter uncertainty and external disturbances are considered simultaneously. The nonlinear disturbance observer gain is selected as $l(x) = \text{diag}([.13, .0032, .0331])$. The simulation results are shown in Fig. 9.
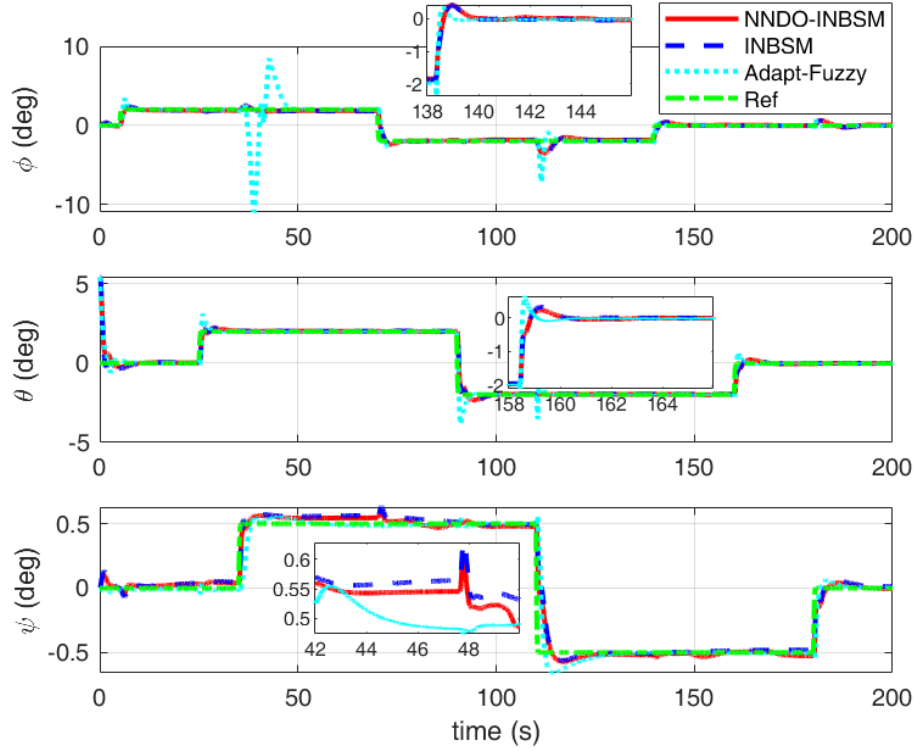
Fig.9. Attitude angle tracking responses under model uncertainty and unknown disturbances

From Fig.9, it can be seen that the adaptive fuzzy control responses also have larger overshoots and errors than those of INBSM and NNDO-INBSM design due to the INBSM introducing the $\dot{x}_{2r}$ feedback and more inputs required for the adaptive fuzzy control. Compared to INBSM, the NNDO-INBSM responses have lower overshoots, which shows that the NNDO-INBSM design has better capability under transient inputs.

Scenario III: actuator faults with model uncertainties and disturbances

This scenario considers actuator faults due to damages and loss of effectiveness. The actuator faults are set as follows

$$\delta_i = (1 - \rho_{f_i}) \times \delta_i^0 \ (i = e, a, r), \tag{85}$$

where $\rho_{f_i} = 0.1$ is the loss effectiveness factor of each actuator, the faults of the elevator, aileron and rudder occur at times of 50s, 80s, and 120s and remain until the end. Model parameter uncertainties and disturbances are also considered as for Scenario II. The nonlinear disturbance observer gain is

selected as $l(x)$ = diag([.25, .005, .01]), the fault estimation estimator parameters are chosen as P_f = diag([1, 1, 60]), γ_f = diag([0.2, 0.02, 0.2]). The simulation results are shown in Figs 10-14.
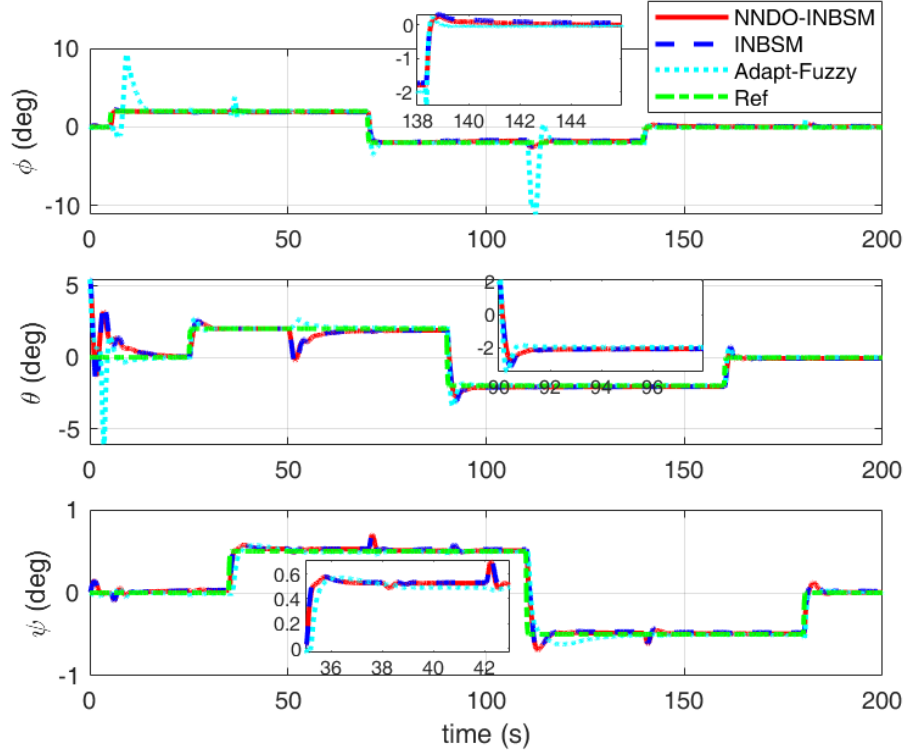

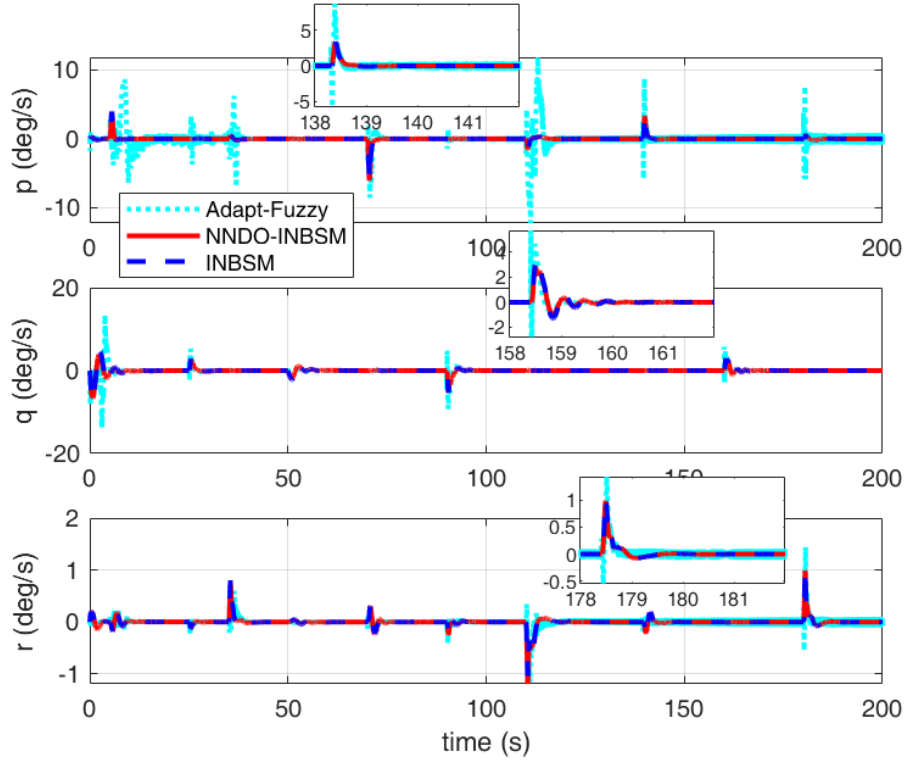Fig.10. Attitude angle tracking responses under faults and model uncertainties

Fig.11. Angular rate responses under faults and model uncertainties

From Figs 10 and 11, it can be seen that the output tracking responses begin oscillating after the actuator faults at 50 and 80sec. The INBSM responses have quicker convergence in roll, pitch and yaw motions than the responses of the adaptive fuzzy control, this shows the INBS design has strong FTC capability. The steady tracking errors for the INBSM and NNDO-INBSM designs are smaller than those of adaptive fuzzy control. Compared with the INBSM control, the tracking responses of the NNDO-INBSM control have smaller overshoots and steady tracking errors, which show that the NNDO-INBSM design has better compensation capability for actuator faults and model uncertainties through the nonlinear disturbance observer. It is noticeable that there will be larger tracking error in both roll and yaw motions if the disturbances cannot be accurately estimated because the $\dot{x}_{2r}$ feedback will amplify the disturbances or the fault inputs.

The disturbances have been observed via disturbance observers as seen in Figs 12 and 13 where it can be seen that observable roll disturbances can be tracked well while those of pitch and yaw motions have more estimation error in the transient process, this results from state varying and actuator faults, but all observable disturbance estimations converge to their true values even for actuator faults. Fig.13 shows that there are large estimation values of INBSM method compared with those of NNDO-INBSM control, which demonstrates that the NNDO-INBSM design can reduce the observable disturbances.
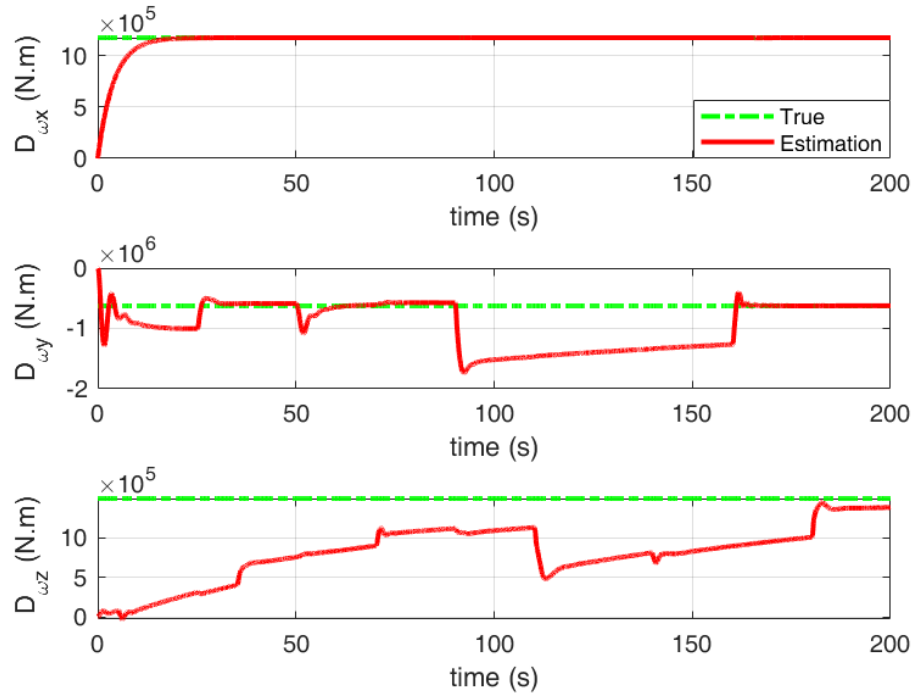
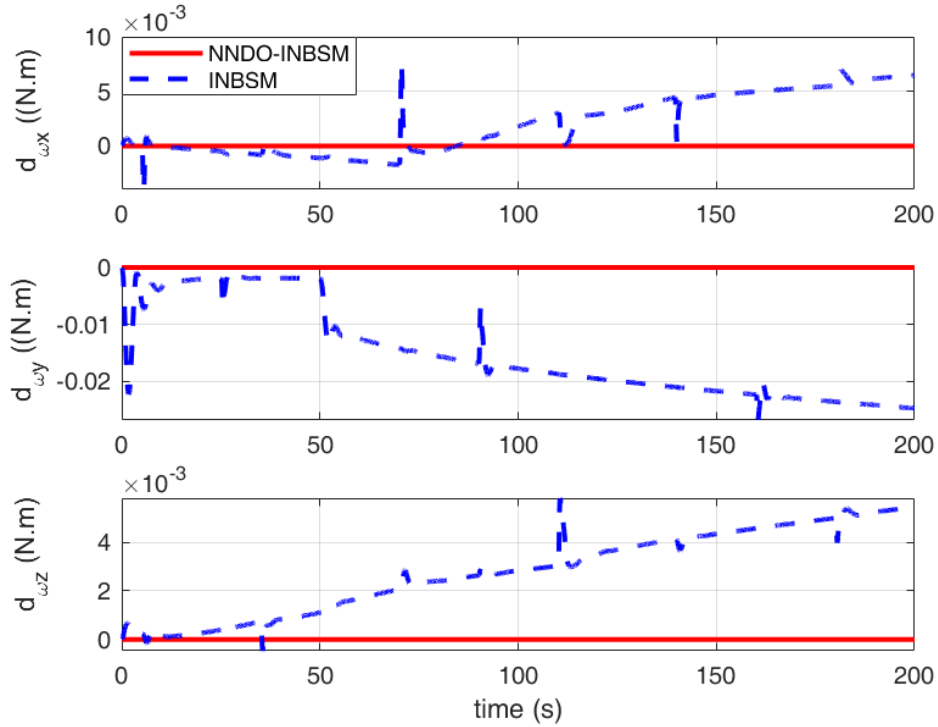Fig.12. Observable disturbance estimation under faults and model uncertainties

Fig.13. Unobservable disturbance approximation under faults and model uncertainties

The actuator fault estimation and actuator output responses are shown in Fig.14 and Fig.15, from which

it can be seen that the actuator angles have been accurately estimated using the fault estimator of (65),

and the NNDO-INBSM has larger inputs than those of INBSM when commands change or there are

input faults. This is because NNDO-INBSM adds a disturbance compensator u_d of (11) and makes the

output tracking responses smoother and quicker. Meanwhile, the adaptive fuzzy control inputs are

bigger than the INBSM and NNDO-INBSM design, this shows that adaptive fuzzy control requires

more control inputs, which makes the actuator saturate more easily when unknown disturbances and
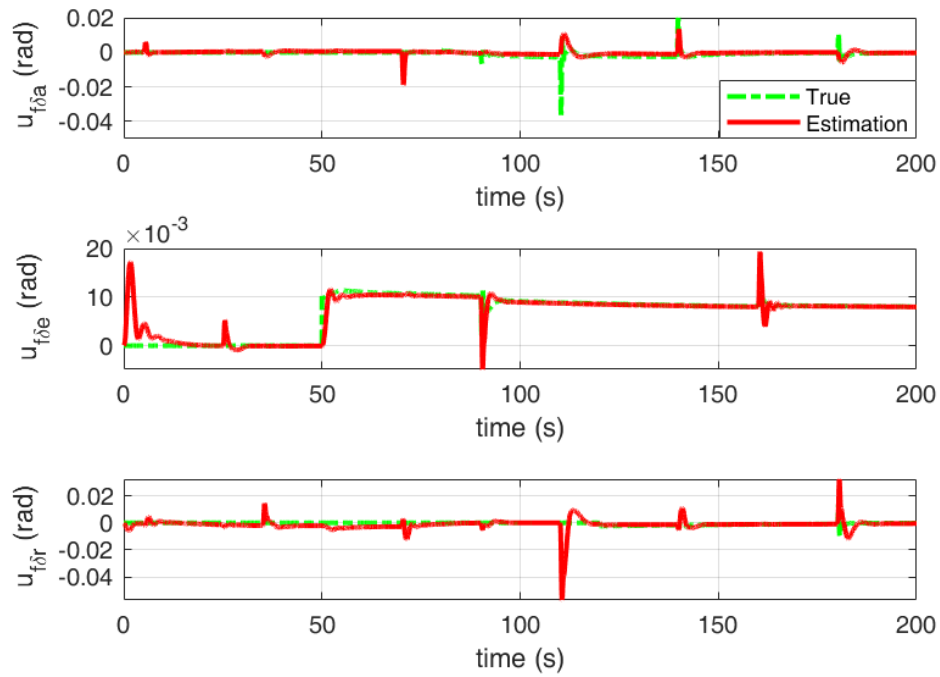
faults occur, see Fig.15.
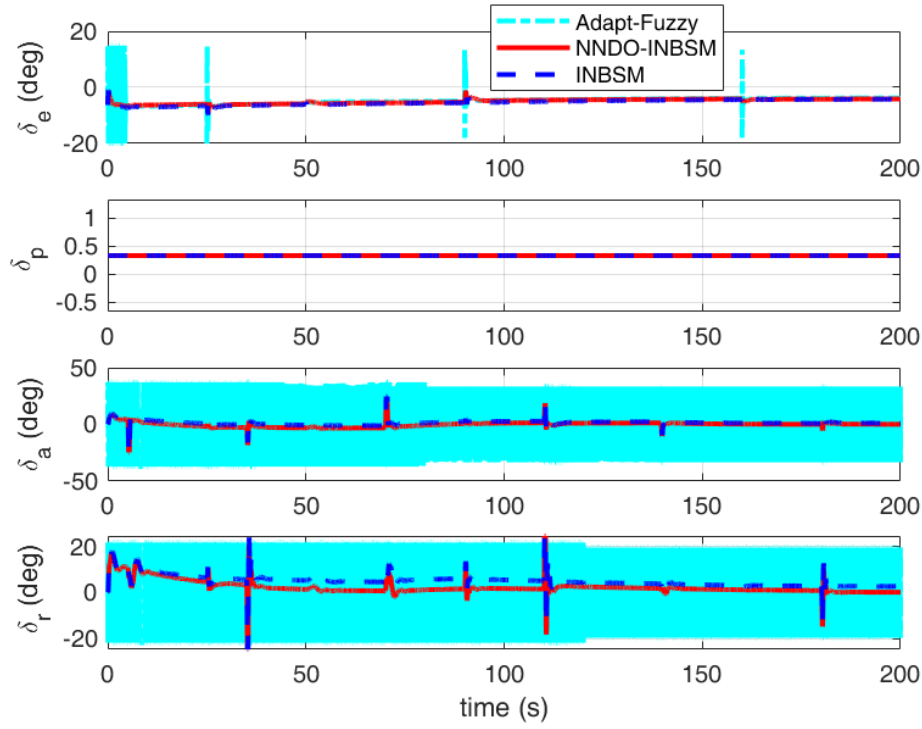

Fig.14. Actuator fault estimation

Fig.15. Actuator responses under faults and model uncertainties

5. **Conclusion**

In this paper we propose the NNDO-INBSM approach for the control of the BWB aircraft. Based on a 3-DOF nonlinear model, an attitude tracking controller is designed. The developed controller stabilizes the attitude and angular rate and enhances the stability of the BWB aircraft via the INBS and INDI methods with stability augmentation system. Furthermore, an NNDO is introduced to estimate the observable disturbances. Stability analysis shows that the closed-loop attitude tracking error dynamics is asymptotically stable. Three scenarios of the different CG position, unknown disturbances, model uncertainties and actuator faults have been simulated and show the proposed NNDO-INBSM control robustness. Compared with adaptive fuzzy control and INBSM controllers, the NNDO-INBSM achieves better attitude tracking performances even though the BWB aircraft is affected by a varying CG position, parametric uncertainties, external bounded disturbances and actuator faults. Therefore, the effectiveness and availability of the NNDO-INBSM design are

demonstrated. Results from the nonlinear simulations confirm that the performance and robustness objectives are achieved. The methodology can be extended to trajectory control.

Acknowledgements

References

[1] M. Carlsson. Control surface response of a blended wing body aeroelastic wind-tunnel model, J. Aircraft, 42(3) (2005) 738-742

[2] S. H. Goldthorpe, K. F. Rossitto, D. C. Hyde, and K. R. Krothapalli. X-48b blended wing body flight test performance of maximum sideslip and high to post stall angle-of-attack command tracking, in AIAA Atmospheric Flight Mechanics Conference, AIAA- 7514, (2010) pp.1-17

[3] V. G. Dmitriev, L. M. Shkadov, V. E. Denisov, B. I. Gurevich, The flying wing concept- Chances and risks, in 2003 AIAA/ICAS International Air and Space Symposium and Exposition: The Next 100 Years, (2003) pp.1-11

[4] X. Xu, and Z.Zhou, Study on longitudinal stability improvement of flying wing aircraft based on synthetic jet flow control, Aerospace Sci and Tech, 46 (2015) 287-298.

[5] M.Kozek, A.Schirrer, Modeling and control for a blended wing body aircraft, Springer, Switzerland. 2014. pp.1-25 (Chapter1).

[6] N.Qin, A.Vavalle, A. L.Moigne, M.Laban, K.Hackett, P.Weinerfelt, Aerodynamic considerations of blended wing body aircraft, Progress Aerosp Sci, 40(6) (2004) 321-343

[7] H. V. Castro, Flying and handling qualities of a fly-by-wire blended-wing-body civil transport

aircraft, PhD thesis, Cranfield University, UK, 2003.

[8] N. U.Rahman, and J. F. Whidborne, Propulsion and flight controls integration for a blended-wing-body transport aircraft, J.Aircraft, 47(3)(2010) 895-903

[9] D.Yann, B. Joël, A. Daniel, C. Toussaint, G. Taquin, Multicontrol surface optimization for blended wing–body under handling quality constraints, J. Aircraft, 55(2), (2018) 638-651

[10] M.Krstic, I.Kanellakopoulos, P.Kokotovic, Nonlinear and adaptive control design, John Wiley &Sons Inc. 1995, (1st edn) pp.29-121

[11] S. Q. Liu, S. J. Gong, Y. X. Li , Z. R. Lu, Vectorial backstepping method–based trajectory tracking control for an under-actuated stratospheric airship, Aeronautical J., 121(1241) (2017) 916-938

[12] S. Q .Liu, Y. J. Sang, Underactuated stratospheric airship trajectory control using an adaptive integral backstepping approach, J. Aircraft, 55(6) (2018) 2357-2371

[13] S. Q .Liu, Y. J. Sang, J. F. Whidborne, Adaptive sliding-mode-backstepping trajectory tracking control of underactuated airships, Aerosp Sci Tech, 97(2020)pp.1-13.

[14] S. Q. Liu, J. F. Whidborne, L. He, Backstepping sliding-mode control of stratospheric airships using disturbance-observer, Advan Space Research, available online: https://www.sciencedirect.com/science/article/pii/S0273117720307778, (2020) pp.1-14.

[15] S. Q. Liu, J. F. Whidborne, Neural network adaptive backstepping fault tolerant control for unmanned airships with multi-vectored thrusters, Proc of the Institution of Mech Eng, Part G: J. Aerosp Eng, available online:https://journals.sagepub.com/doi/10.1177/0954410020976611, (2020) pp.1-14.

[16] B. J.Bacon, A. J. Ostroff, Reconfigurable flight control using nonlinear dynamic inversion with a

special accelerometer implementation. In AIAA Guid, Nav, and Contr Conf and Exhibit, Denver, CO, AIAA-2000-4565, (2000) pp.1-15

[17] S.Sieberling, Q. P.Chu, J. A.Mulder. Robust flight control using incremental nonlinear dynamic inversion and angular acceleration prediction, J. Guid Contr& Dyn, 33(6) (2010)1732-1742

[18] E. J. J.Smeur, Q. Chu, , G. C. H. E. D Croon. Adaptive incremental nonlinear dynamic inversion for attitude control of micro air vehicles, J. Guid Contr& Dyn, 39(3) (2016) 450-461

[19] P. Lu, , E. J. V. Kampen, , C. D.Visser, Q. P. Chu, Aircraft fault-tolerant trajectory control using incremental nonlinear dynamic inversion, Contr Eng Prac, 57 (2016) 126-141.

[20] X.Wang, E. J. V. Kampen, Incremental backstepping sliding mode fault-tolerant flight control, AIAA SciTech Guid Nav and Contr Conf, San Diego, CA, (2019) pp.1-16

[21] P.Acquatella, E. J. V. Kampen, Q. P. Chu, Incremental backstepping for robust nonlinear flight control, in Proc of the EuroGNC 2013, 2nd CEAS Specialist conf on Guid, Nav & Contr, Delft University of Technology, Delft, Netherlands, (2013) 1444-1463

[22] A. A. H. Ali, Q. P. Chu, E. J. V.Kampen, C. C. de Visser, Exploring adaptive incremental backstepping using immersion and invariance for an F-16 aircraft, in AIAA Guid, Nav, and Contr (GNC) Conference, AIAA 2014-0084, (2014) pp 1-31

[23] P. Lu, E.V. Kampen, Q. Chu, Robustness and tuning of incremental backstepping approach, in AIAA Guid, Nav, & Contr Conf, AIAA Paper 2015-1762 (2015) pp.1-15

[24] Y. C.Wang, W. S.Chen, S. X.Zhang, J. W. Zhu, L. J.Cao, Command-filtered incremental backstepping controller for small unmanned aerial vehicles, J. Guid Contr & Dyn, 41(4) (2008) 450-461

[25] W.H. Chen, J. Yang, G. Lei, S. Li, Disturbance observer-based control and related methods: an

overview, IEEE Trans Industr Elec, 63(2) (2015)1083–1095.

[26] Y. Oh, W. K. Chung, Disturbance-observer-based motion control of redundant manipulators using inertially decoupled dynamics, IEEE/ASME Trans Mechatronics, 4(2) (1999)133–145

[27] A.J. Ammar, B. Shirinzadeh , M. Ghafarian , T. K. Das , Y. Tian , D. Zhang, A fuzzy disturbance observer based control approach for a novel 1-DOF micropositioning mechanism, Mechatronics 65 (2020) 102317,pp.1-15

[28] M. Chen, Y.L. Zhou, W. W. Guo, Robust tracking control for uncertain MIMO nonlinear systems with input saturation using RWNNDO, Neurocomputing, 144 (2014) 436–447

[29] Z.W. Zheng, L Sun, Path following control for marine surface vessel with uncertainties and input saturation, Neurocomputing, 177 (2016)158–167

[30] W. H. Chen, D. J. Ballance, P. J. Gawthrop, J. O'Reilly, A nonlinear disturbance observer for robotic manipulators, IEEE Trans. Industr Electron, 47(4) (2000) 932-938.

[31] Y. M.Zhang, J. Jiang, Integrated design of reconfigurable fault tolerant control systems, J. Guid, Contr, and Dyn, 24 (1) (2001)133-136

[32] B. L.Stevens, F.L. Lewis, E.N. Johnson, Aircraft Control and Simulation, John Wiley & Sons, Inc. 3rd. 2016, pp. 287-289

[33] X. Jin, Adaptive fault tolerant control for a class of input and state constrained MIMO nonlinear systems, Int J. Robust & Nonlinear Contr, **26** (2016) 286-302.

[34] H. K. Khalil, Nonlinear Systems, Prentice Hall Press, 3rd. 2002; pp. 124

[35] L. X. Wang, Adaptive Fuzzy Systems and Control. Englewood Cliffs, NJ, USA: Prentice-Hall, 1994.

[36] Y. M. Li, K. K. Sun, and S.C. Tong, Observer-based adaptive fuzzy fault-tolerant optimal control

for SISO nonlinear systems, IEEE Trans. on Cybernetics, 49(2) (2019) 649-641

[37] S.C. Tong , K.K. Sun , and S. Sui, Observer-based adaptive fuzzy decentralized optimal control design for strict-feedback nonlinear large-scale Systems, IEEE Trans. on Fuzzy Sys, 26(2) (2018) 569-584

CRediT author statement

Roles of the authors,

Shiqian Liu: Methodology, control design and Simulation, Writing- Original draft

James F. Whidborne: Conceptualization, BWB aircraft model, Writing- Reviewing and Editing

Dr. **Shiqian Liu**　　　Prof. **James F. Whidborne**

Declaration of interest statement

We declare that we have no financial and personal relationships with other people or organizations that can inappropriately influence our work,

there is no professional or other personal interest of any nature or kind in any product, service and /or company that could be construed as influencing the position presented in, or the review of, the manuscript entitled.

Best Regards

Shiqian Liu, James F. Whidborne

2021-08-19

Observer-based incremental backstepping sliding-mode fault-tolerant control for blended-wing-body aircrafts

Liu, Shi Qian

Elsevier